Activation of Primary Alcohols via Metal Ligand Cooperation in ($^{Ph}I_2P^{2-}$)AlH and the Synthesis and Characterization of Redox Active Ligand Complex [$(cat)_2Si(catH)$][Et_3N]

By

MEGAN L. MCKENNEY

B.S. Chemistry (Eckerd College) 2011

THESIS

Submitted in partial satisfaction of the requirements for the degree of

MASTERS OF SCIENCE

in

CHEMISTRY

in the

OFFICE OF GRADUATE STUDIES

of the

UNIVERSITY OF CALIFORNIA

DAVIS

Approved:

_____

Dr. Louise A. Berben, Chair

_____

Dr. Philip P. Power

_____

Dr. Frank E. Osterloh

Committee in Charge

2014

ProQuest LLC.
789 East Eisenhower Parkway
P.O. Box 1346
Ann Arbor, MI 48106 - 1346

Acknowledgements

I would like to thank UC Davis and Dr. Louise Berben for funding. I would also like to thank Dr. Phil Power and Dr. Frank Osterloh for serving on my thesis committee. To Shelly Archer, who has been so helpful all of my years here.

I would like to extend my thanks to all of my lab mates, especially Thomas Myers for his encyclopedic knowledge of synthesis and extra aid in X-ray crystallography. A huge thanks to Pauline Serrano for both academic and emotional support, lab dance parties, OOVDs, and lots of laughs.

I'd like to extend my gratitude to the UC Davis Chemistry Dept. faculty, but especially Dr. Kym DeCesare, Dr. Matt Augustine, and Dr. Don Land. Thanks for all of the good advice and fun times, both on campus and on the coast.

I would also like to thank my wonderful friends who have been so supportive and made all of the tough times easier, especially my long-time friends Max, Carina, Katie, Alex, Melissa, and Brant. Thanks for always having my back no matter what. An extra special thanks to my fellow chemist and best friend Laura McWade, who has become more like the sister I never had. Thank you for your never ending support and all of the epic adventures we've embarked on. You are a true R.O.D.B.

A huge thank you to my family: Mom, Ed, Eric, and my Werner. To my CA family, Sharon and Pete for support, love, and fun times. An extra special thanks to my mom: a tough, smart, and beautiful woman who has always lent me her ear and given great advice. I love you all.

A final thank you to the haters, it was great motivation.

Table of Contents

Abstract

The oxidative addition of primary alcohols (phenol, *tert*-butyl alcohol, benzyl alcohol, methanol, 1-octanol) via ($^{Ph}I_2P^{2-}$)AlH ($^{Ph}I_2P$ = bis(imino)pyridine) was investigated for production of the corresponding aldehyde with elimination of H_2. The primary alcohols utilized with β-hydrogen available (benzyl alcohol, methanol, and 1-octanol) were also investigated for catalytic turnover of H_2 and the simultaneous production of its respective aldehyde. Phenol and *tert*-butyl alcohol reacted with the ($^{Ph}I_2P^{2-}$)AlH complex to afford ($^{Ph}I_2P^{-}$)AlH(OC_6H_5) and ($^{Ph}I_2P^{-}$)AlH(OC_4H_9), respectively. The reaction of ($^{Ph}I_2P^{2-}$)AlH with benzyl alcohol successfully afforded H_2 and benzaldehyde in the presence of excess benzyl alcohol, however no evidence for the reaction was obtained.

The synthesis and characterization of the novel silicon compound [$(cat)_2Si(catH)$][Et_3N] (cat = 3,5-di-*tert*-butylcatechol) is reported. Its solid state structure revealed a third protonated "cat" ligand bound to the 5th coordination site of the silicon atom. A different catechol ligand, 2,4-di-*tert*-butyl-6-(*tert*-butylamino)phenol (apH_2), was also synthesized in an effort to metallate with silicon. No silicon complexes were obtained and it can be speculated that since the silicon atom is relatively small, the bulkier ligand framework could not bind to afford a stable 4 or 5- coordinate silicon (IV) species.

Abbreviations and Notations Used in the Text

C_1 = an organic molecule that only contains 1 carbon atom

$^{Ph}I_2P$ = bis(imino)pyridine ligand

THF = tetrahydrofuran

NMR = nuclear magnetic resonance

ppm = unit for NMR chemical shifts, parts per million

GC = gas chromatography

MS = mass spectroscopy

TCD = thermal conductivity detector

TON = turnover number, quantity usually expressed as (moles product produced/ moles catalyst used)

MeOH = methanol

MeCN = acetonitrile

'cat' = 3,5- di-*tert*-butylcatechol

apH_2 = 2,4- di-*tert*-butyl-6-*tert*butylaminophenol

Introduction

1.1 Motivation:

In recent years, there has been an increasing interest in developing new technologies which will permit the production of an alternative, non-petroleum based carbon fuels, such as methane, methanol, or the likes there of, from plentiful carbon sources such as carbon dioxide (CO_2).[1] Replacement feedstock would also be useful for catalytic reactions as well as a replacement for carboxylation reagent.[2] Those reactions, which make use of CO_2 as a feedstock material, have dual advantages of employing a cheap, abundant source of carbon while also being considered carbon neutral. The combustion of organic products generated from these reactions would simply regenerate the CO_2 used to initially synthesize the feedstock material.

With the increased level of concern regarding climate change due to the use and burning of fossil fuels and the accumulation of CO_2 in the atmosphere, it is an obvious, yet challenging goal to develop a carbon neutral chemical process to generate a renewable fuel source. However, without an effective catalyst for the previously suggested reactions, they remain too energetically demanding to be a practical on an industrial scale. Efficient, low energy processes for either the transformation of small molecules, or for the generation of H_2, are attractive goals for the general and industrial communities.

An important and emerging goal of sustainable chemistry is the investigation of earth abundant main group metal alternatives to precious transition metal catalysts.[3] The use of base-metal catalysts is advantageous for industrial applications, but the use of expensive transition metals makes the feasibility of some of these processes

questionable. Other challenges that catalysis is facing today are the replacement of traditional synthetic processes that generate waste with sustainable catalytic reactions that create less toxic byproducts. Aluminum is one of the most inexpensive and abundant elements on Earth[4] and consists of approximately 8.3% of the Earth's crust. Aluminum costs approximately $0.89 per pound while price of palladium is $1400 per ounce,[5] making it an extremely cost efficient and environmentally friendly option for our research interests.

1.2 Redox Chemistry: Redox Active ligand Group 13 Complexes, Particularly Aluminum

The use of redox active ligands with main group elements give chemists the ability to explore and mimic aspects of redox chemistry that have previously only been known for transition metals and afford redox reactivity different from that of transition metals.[6] The transition metals have an ability to access multiple oxidation states and form stable complexes, whereas main group elements are usually most stable in one oxidation state (some examples are: Sn, Tl, Pb, Bi, S, P, and potentially Ga and Ge are stable in two oxidation states, found in salts).[7] For *p* block elements, this observation can in part be explained by the lack of empty *d* orbitals. In some typical redox-active transition metal complexes, the redox-active ligand acts as an electron reservoir by facilitating inner-sphere charge redistribution with the metal center. This "non-innocent" behavior is due to the mixing between energetically similar metal *d* (π) and ligand *p* (π) orbitals. In some cases, the orbital mixing can result in intra-molecular electron transfer to general changes in the formal oxidation state of the metal and the ligand.[8] Having a redox- active

ligand aids in providing a "home" for the electron that the main group central atom may not have available in its own set of *p* orbitals.[9] Even though transition metals undoubtedly undergo interesting and notable chemistry, some have negative aspects for instance their cost and low abundance (not including elements like Fe and Co), especially when compared to main group elements. The main group metal ions like the late *d*-block ions like Cu (I), Cu (II), Zn (II), and main group Al (III) and Si have Lewis acidic properties, making them excellent contenders for small molecule activation chemistry.[10] More details will be given in Chapter 2 concerning aluminum centered redox active complexes and the reactivity that has been observed concerning metal-ligand cooperation.

1.2.1 Pincer Complexes and Ligand Cooperation:

Pincer-type complexes are a large family of extremely important compounds in organometallic chemistry. They play key roles in several different chemical transformations such as catalysis, bond activation, mechanistic studies, and the design of new and useful materials.[11,12] Traditionally, pincer ligands were desgined to be stable and unchanged during stoichiometric and catalytic reactions. However, in some cases the ligand itself is capable of undergoing transformation that aid or expand the reactivity of the metal complex.[13] The idea of the "non-innocence" of a ligand, where a redox active ligand participates in the transformation, is a rapidly growing area of interest in organometallic chemistry. Transition metal complexes of bulky, electron rich, "pincer" ligands have important applications in synthesis, bond activation, and catalysis.[14,15] Electron donating, pyridine-based pincer ligands can stabilize coordinatively unsaturated metal complexes.[16] It has been discovered that new modes of metal-ligand cooperation

involving aromatization-dearomatization processes, will lead to unusual bond activation processes and novel environmentally conscious catalysis.[13]

The Milstein group reported a PCP and a PCN pincer ligand that demonstrates C-H agostic coordination, N-arm hemiliability, and the collapse and regeneration of the ligand during reaction (PCP/PCN are *bis*-phospine chelating ligands; the letter describes the atom binding to the metal center from the ligand). These ligands illustrate the metal ligand cooperation by dearomatization of the pincer ligand as a key participant in various catalytic reactions.[17,18,19,20,21] Beginning in the early 2000's, complexes based on "cooperating" ligands have demonstrated notable catalytic activity. It is already known that with most reactions that are catalyzed by metal complexes, the catalytic activity is metal based. The ligands, which can affect the properties of the metal center, do not usually undergo any bond making, bond breaking, or act as an active participant in the catalytic cycle themselves. However, the ligands can undergo reversible structural changes in the process of substrate activation or formation of the product.[22] This acts as a "cooperating" feature with the metal center during a catalytic cycle, such as in the example of hydrogenation of polar bonds. The classical mechanism of hydrogenation involves an inner sphere hydride transfer.[23] This transfer involves the substrate binding directly to the metal center. The coordination in the inner coordination sphere allows for electrophilic activation of the carbon of the carbonyl or imine group by the metal ion, allowing a *cis* hydride ligand to migrate to the β carbon to the metal.[21]

Scheme 1-1: Inner-sphere transfer hydrogenation monohydride mechanism.[2]

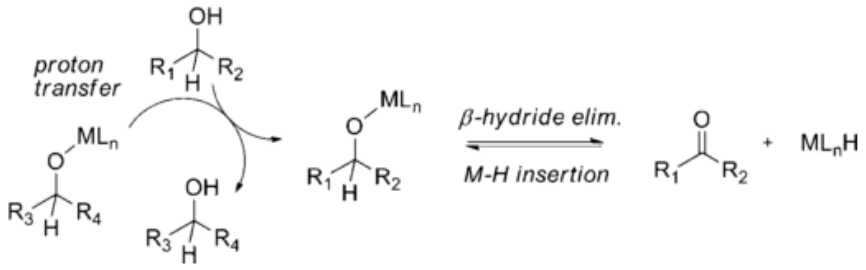

Noyori and coworkers demonstrated the non-classical mechanism for the reduction of polar bonds via ruthenium complexes.[24] In contrast, to the classical inner sphere mechanism; the reduction operates by the hydride transfer to the substrate in the outer coordination sphere of their ruthenium complex. The carbon in either a C=N or C=O bond has a low hydride affinity, making it necessary for an additional electrophile. This could be an external electrophile (HO or TO) or an internal electrophile attached to an ancillary ligand (HOL or TOL). Noyori et al. named this process " metal-ligand bifunctional catalysis" referring to the catalytic systems using the HOL or TIL mechanisms (H being hydrogenation of substrate by use of hydrogen gas, T being hydrogenation of substrates via transfer hydrogen from the hydrogen donor; I being inner sphere, O being outer sphere, and L showing ligand assistance in hydrogen transfer).[25] In a ligand assisted mechanism, the catalysts must have an ancillary ligand *cis* to the hydride to assist in the hydride transfer step in the mechanism. It is necessary for the ligand to have a NH or OH group or an associated electrophile.[23] A flowchart summarizing the classification method is below (Figure 1-1).

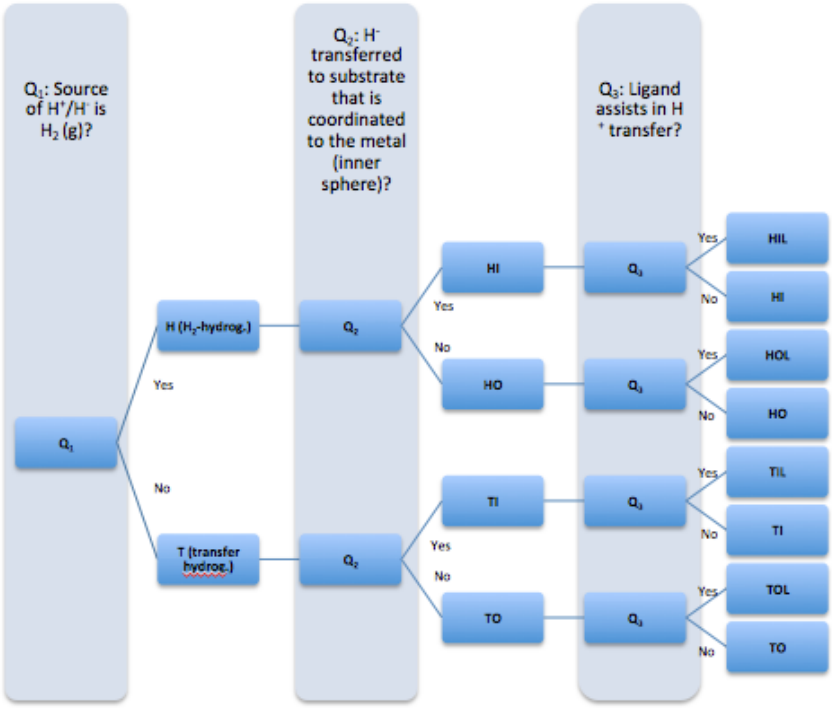

Figure 1-1: A flowchart to classify the mechanisms of the reduction of polar bonds, where H is hydrogenation, T is transfer hydrogenation; I is inner sphere, O is outer sphere; L is ligand assisted.[27]

1.2.2 Bond Activation Chemistry and Net Oxidation of Alcohols:

Traditional organic bond activation requires reactive leaving groups and creates wasteful byproducts, however, inorganic bond activation catalysis removes the necessity of those wasteful synthetic steps and introduces a functionality into the bonds that have not been activated.[26] While bond activation is not a novel idea of modern chemistry, its role in the catalytic cycle of producing H_2 gas and useful organic byproducts has become of indefinite interest in organometallic chemistry.

By replacing highly reactive reagents such as RBr or ROTs with less reactive reagents like ROH or RH, chemists could have access to new and cheaper chemical processes. In the reactions discussed within chapter 2, the substrate is activated and is followed by a bond-constructing step.

These desired steps usually occur with one single catalyst, or two catalysts working concurrently under "one-pot" synthetic conditions.

Alkane, amine, and alcohol activations are established organic mechanisms and have been investigated in several ways.[27,28,29,30,31] Most recently, Berben and coworkers reported an aluminum pincer-type complex employing metal-ligand cooperation with a redox-active ligand.[32] It was found that a bis(imino)pyridine complex of aluminum can activate amine N-H bonds through a metal-ligand cooperative mechanism.

Alcohol dehydrogenation produces aldehydes or ketones, which can also be reactive or coupled with other nucleophiles. By dehydrogenating alcohols to their more reactive aldehyde or ketone oxidation product, subsequent bond construction steps are possible that would not have been possible for the parent alcohols. This type of transformation has been referred to as a hydrogen auto-transfer process, hydrogen borrowing method, or hydrogen transfer.[33] Several groups have demonstrated many useful examples of alcohol activation. The noted leaders of generalizing the method for many different types of transformations and formalizing the concept itself are Fujita and Yamaguchi,[33] Ramón and Yus,[34] and Williams.[35a,35b]

The earliest reported examples of hydrogen transfer date back over 100 years. Early development of hydrogen transfer in the context of alcohol oxidation including the framework of homogenous transition metal processes notes Oppenauer's report of aluminum *tert*-butoxide oxidation of secondary alcohols into ketones. Several groups have demonstrated that transition metal catalyzed systems that show Oppenauer-type alcohol oxidation reactivity. The transition metals typically seen in the first catalysts described to have the hydrogen transfer capabilities from alcohols to carbonyls were

iridium, rhodium, and ruthenium. All of these catalysts tend to require harsh conditions for any notable conversion.[36,37,38,39,40] All of the for mentioned catalysts are found to need a basic condition to serve as an activator of the hydrogen transfer catalysts as well as a promoter for the reaction itself.

Besides hydrogen transfer, the other oxidative path for alcohols is the extrusion of H_2. While the hydrogen that is removed is no longer available to the system, this mode of oxidation avoids any need of a stoichiometric oxidant. For example, esters can be formed an alcohol following this method. In the Tischenko process, esters are formed from the dimerization of the aldehydes, which is catalyzed by the metal complex, lanthanide alkoxides, or alkali alkoxides.[41] The reactivity of the metal complexes for the Tishchenko reaction mimics the reactivity for ester formation via the oxidative activation and dimerization of alcohols (Figure 1-2). [41]

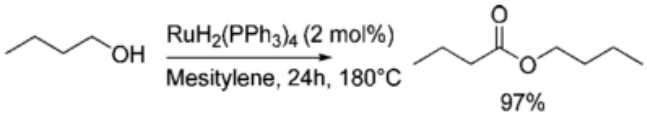

Figure 1-2: Oxidative Esterification of Primary Alcohols.[41]

The dihydride $[RuH_2(PPh_3)_4]$ is a known Tishehenko reaction catalyst. It is also known to have the ability to form esters and lactones from the dehydrogenative activation of alcohols. Murahashi later disagreed with the suggestion that the alcohol esterification reaction operates through a Tishchenko mechanism due to the complex's inability to form ester product in substantial yeild from aldehydes under the alcohol esterification conditions.[41] Shvo's complex, $[(\eta^4\text{-}C_4Ph_4CO)Ru(CO)_3]_2$ proved capable of Tishchenko reactions as well as oxidation esterification.[42,43] It is capable of ester and lactone formation at elevated temperatures in the absence of base. Another ruthenium complex

capable of performing an oxidative esterification is the PNN pincer complex developed by Milstein and co-workers.[21, 44, 45] They reported this complex that gives dehydrogenation of primary alcohols to esters in the absence of a base. Two alcohols can form other products besides esters in a dehydrogenative activation. Milstein and coworkers reported the formation of acetals upon reaction of alcohols with ruthenium PNP pincer complex with an extrusion of H_2.[45] Neutral conditions lead to the acetal formation; the addition of base promotes ester formation (Figure 1-3).

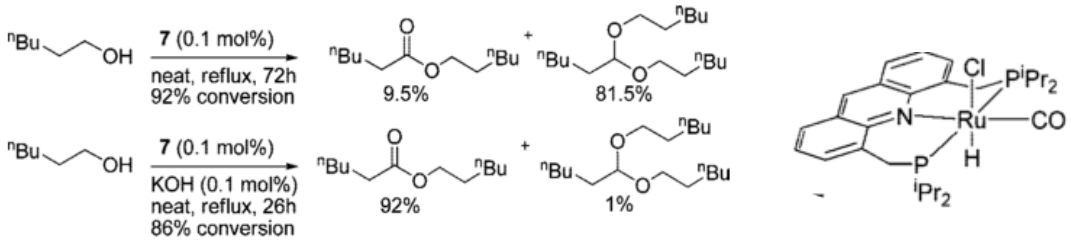

Figure 1-3: Left: Base dependent selectivity in an acetal and ester formation including the loss of H_2 as another product; Right: Ruthenium centered PNP pincer complex.[43]

Redox active aluminum complexes' ability to catalyze alcohol dehydrogenations has not been extensively explored. Investigating the capability of a redox active aluminum complex in the dehydrogenation of alcohols seems reasonable and promises a more sustainable method, since it would not require the addition of a base to promote the aldehyde or ester formation. Alcohol dehydrogenation traditionally requires a base, and since there is less reported on synthetic routes that negate the need for base addition, there will be no shortage of interesting chemistry to report on alcohol activation utilizing aluminum.

1.3 FLP Chemistry

The combination of Lewis donors and acceptors in which the steric demands preclude formation of the simple adduct are dubbed "frustrated Lewis pairs" or FLPs.

Lewis acids are characterized by low lying lowest unoccupied molecular orbitals (LUMOs) which can interact with the lone electron pair in the high lying highest occupied molecular orbital (HOMO) of a Lewis base. Instead of forming water when mixing the Lewis acid and the Lewis base, the combination results in the formation of a Lewis acid/base adduct or FLP. The "frustration" leaves an unquenched acidity and basicity that the systems have been reported to prompt non-classical and in some cases unparalleled reactivity.[46,47]

Typical examples of frustrated Lewis pairs are inter- or intramolecular combinations of bulky phosphines or amines with strongly electrophilic $RB(C_6F_5)_2$ components. Several examples of FLPs are able to cleave dihydrogen heterolytically.[46] The resulting H+/H- serves as active metal-free catalysts for the hydrogenation of bulky imines, enamines, and enol ethers. FLPs have also been reported to react with alkenes, aldehydes, and a variety of other small molecules, including carbon dioxide in cooperative reactions, all offering new strategies for synthetic organometallic chemistry like conversion of CO_2 to CH_4.[47] The use of strongly donating ligands, combined with large steric bulk, will prevent bond formation.

Mentioned previously, transition metal complexes supported by redox-active ligands have gained much attention recently for many attractive qualities. In these complexes, the ligand demonstrates non-innocent behavior that arises from mixing energetically similar π orbitals,[48] which has established the ability to change the oxidation state of both the ligand and the metal by electron transfer.[49]

When beginning the initial investigation of frustrated Lewis acids and bases, the necessary steric bulk to preclude formation must be considered. Stephan and coworkers

reported a borenium and boryl-phosphonium resonance created from B-H activation of their catechol borane.[50] The backbone of their cation is similar to that of a catechol. The catechol has several attractive advantages with metal ions and coordination chemistry, as well as redox chemistry. Redox activity is an attractive characteristic for the silicon FLP chemistry since one goal is to produce a neutral five coordinate silicon compound while keeping silicon in a stable oxidation state. A substituted catechol, like 3,5-ditertbutylcatechol, gives favorable steric hindrance. Other substitutions at the 1 or 2 position, like amines, can also tune the reactivity of the complex to have favorable stability and can improve catalytic activity of certain complexes.[51] Stephen and Erker have taken a very elegant approach towards transforming CO_2 and other small molecules.[52] Stephan showed that CO_2 can be trapped via insertion into an adduct formed between $AlCl_3$ and $PMes_3$. Another established FLP used $B(C_6F_5)_3$ and the sterically encumbering secondary phosphine $(C_6H_2(CH_3)_3)PH$. This reaction forms an adduct between the Lewis acid and base and liberates H_2 from the complex.[53a,53b] An example of the fixation of CO_2 with FLPs is the formation of $^tBu_3P(CO_2)B(C_6F_5)_3$ from exposing a solution of $(C_6F_5)_3$ and P^tBu_3 to CO_2 gas.[54]

1.3.1 Investigations of Silicon for Redox Active Compounds

The foremost difficulty with main group elements is that multiple oxidation states of the metal are not readily accessible as they are with transition metals. A strategy that can be used to mimic the transition metal-like redox behavior with main group elements is to utilize *N*-donor redox active ligands into the metal-ligand framework of the main group complexes. Redox active ligands have shown significant amounts of interesting chemistry incorporating group 13 elements. Within the Berben group, focus has remained

on aluminum and gallium, both in the 3^+ oxidation states for FLP investigations thus far. Another relatively abundant and inexpensive main group element to consider for complexation is silicon. Silicon is most commonly found in its stable oxidation states of 2^+, seen in silicon carbine compounds, or 4^+ found in silicon oxides. The ionic radius of Si^{4+} is almost equivalent to the ionic size of Al^{3+} (0.041nm versus 0.050 nm, respectively).[55] Silicon has shown to be a valuable precious metal alternative that allows for the tuning of its electrophilicity. Silicon has been reported to coordinate small molecules and form six coordinate silicon compounds as well as stabilize non-innocent ligands in their reduced states.[56, 57] Recently there has been reports of 5 coordinate heterocyclic silicon compounds capable of bond activation as well.[58] The difficulty in synthesizing novel 4 or 5 coordinate silicon (IV) compounds is that Si^{4+} containing reactions can generate challenging Si^{2+} and Si^{3+} intermediates, that may even inhibit a intended synthetic pathway. There are five coordinate chelated silicon compounds reported that are stabilized by a salt, however, the synthetic route to the compound is not sustainable in its cost, time, or waste.[59] Of FLPs reported to have the ability to activate small molecules, silicon centered complexes have not been widely investigated. Since less is known about silicon's potential as an activator of small molecules or its participation in catalytic cycles involving FLPs (without being a sacrificial reductant), further investigation of silicon centered FLPs is promising.

Using redox active ligand systems, chemists have shown that transition metal character can be imparted to the main group elements, as well as revealed abilities reserved to the main group elements. Such ligands have the ability to form stable compounds with *p*-block elements and partake in interesting chemistry. The field of

redox active main group/organometallic chemistry is continually growing and remains to be explored in the near future. The usefulness of these complexes in catalytic cycles, as well as their overwhelming potential to be used as new reagents are areas that will need to be investigated further. This chemistry promises no shortage of interesting reactivity to report in the upcoming years.

References:

[1] Benson, E. E.; Kubiak C. P.; Sathrum A .J.; Smieja, J. M. *Chem. Soc. Rev.* **2009**, *38*, 89.

[2] Riduan, S. N.; Zhang, Y. *Dalton Transactions* **2010,** *39,* 3347.

[3] *Catalysis without precious metals;* Bullock, R.M., Ed.; Wiley,-VCH: Hoboken, NJ, 2010.

[4] Suess, H.; Harold, U. *Reviews of Modern Physics* **1956,** *28,* 53.

[5] London Metal Exchange, www.lme.com; September 22nd , 2013.

[6] *Introduction to Coordination Chemistry;* Lawrance, G. A.; Wiley & Sons: New York. 2003

[7] Pierpont, C. G.; Lange, C. W. *Prog. Inorg. Chem.* **1994**, *41*, 381.

[8] Attia, A. S.; Pierpont, C. G. *Inorg. Chem.* **1998**, *37*, 3051.

[9] Power, P. P. *Chem. Rev.* **2003,** *103*, 789..

[10] Wright, A. M.; Wu, G.; Hayton, T. W. *J. Am. Chem. Soc.* **2010,** *132,* 14336.

[11] Hartley F. R.; Patai S. (Eds) *The chemistry of the metal-carbon bond the structure, preparation, thermochemistry, and characterization of organometallic compounds*, Volume 1. **1982**, Wiley, New York.

[12] Dyke, A. M.; Hester, A. J.; Lloyd-Jones, G. C. *Synthesis* **2006,** *24,*4093.

[13] Poverenov, E.; Milstein, D. *Top Organomet. Chem.* **2013,** *40,* 21.

[14] Morales-Morales, D.; Jensen, C. M, Eds. *The Chemistry of Pincer Compounds,* Elseiver; Amsterdam, 2007.

[15] Albrecht, M.; Van Koten, G. *Angew. Chem. Int. Ed.* **2001,** *40,* 3750.

[16] van der Vlugt, J. L.; Reek, J. N. H. *Angew. Chem. Int. Ed.* **2009,** *48,* 8832.

[17] Gnanaprakasam, B.; Milstein, D. *J. Am. Chem. Soc.* **2011,** *133*, 1682.

[18] Gnanaprakasam, B.; Ben-David, Y.; Milstein, D. *Adv. Synth. Catal.* **2007,** *352,* 3169.

[19] Gunanathan, C.; Ben-David, Y.; Milstein, D. *Science* **2007,** *317,* 790.

[20] Balaraman, E.; Gnanaprakasam, B.; Shimon, L.J.W.; Milstein, D. *J. Am. Chem. Soc.* **2010,** *132,* 16756.

[21] Zhang, J.; Leitus, G.; Ben-David, Y.; Milstein, D. *J. Am. Chem. Soc.* **2005,** *127,* 10840.

[22] Guananathan, C.; Milstein, D. *Acc. Chem. Res.* **2011,** *44,* 588.

[23] Milstein, D. *Top. Catal.* **2010**, *53,* 915.
[24] Noyori, R.; Hashiguchi, S. *Acc. Chem. Res.* **1997,** *30,* 97.
[25] Clapham, S. E.; Hadzovic, A.; Morris, R. H. *Coord. Chem. Rev.* **2004,** *248,* 2201.
[26] Zhang, J.; Gandelman, M.; Shimon, L. J. W.; Rozenberg, H.; Milstein,D. Organometallics 2006, 23, 4026.
[27] Dobereiner, G. E.; Crabtree, R. H. *Chem. Rev.* **2010,** *110,* 681-703.
[28] Crabtree, R. H.; Milhelcic, J. M.; Quirk, J. M. *J. Am. Chem. Soc.* **1979,** *101,* 7738.
[29] Janowicz, A. H.; Bergman, R. G. *J. Am. Chem. Soc.* **1982**, *104,* 352.
[30] Murahashi, S.; Komiya, N.; Terai, H.; Nakae, T. *J. Am. Chem. Soc.* **2003**, *125,* 15312.
[31] Gu, X-Q. G.; Chen, W.; Morales-Morales, D.; Jensen, C. M. *J. Mol. Catal. A : Chem.* **2002**, *189,* 119.
[32] Myers, T. W.; Berben, L. A. *J. Am. Chem. Soc.* **2013**, *135,* 9988.
[33] Fujita, K.; Yamaguchi, R. *Synlett* **2005**, 560.
[34] Ramon, D. J.; Yus, M.; Guillena, G. *Angew. Chem. Int. Ed.* **2007**, *46,* 2358.
[35] (a) Hamid, M. H. S. A.; Slatford, P. A.; Williams, J. M. J. *Adv. Synth. Catal.* **2007**, *349,* 1555. (b) Nixon, T. D.; Whittlesey, M. K.; Williams, J. M. J. *Dalton Trans.* **2009**, 753.
[36] Oppenauer, R. V. *Recl. Trav. Chim. Pay-Bas.* **1937**, *56,* 137.
[37] Svoboda, P.; Hetfleys, J. *Collect. Czech. Commun.* **1977**, *42,* 2177.
[38] Haddad, Y.; Blum, J. *Tetrahedron Lett.* ***1964****, 361.*
[39] Camus, A.; Mesroni, G.; Zessinovich, G. *J. Mol. Catal.* **1979**, *6,* 231.
[40] Grigg, R.; Mitchell, T. R. B.; Sutthivaiyakit, S. *Tetrahedron* **1981**, *37,* 4313.
[41] Murahashi, S. I.; Naota, T.; Ito, K.; Maeda, Y.; Taki, H. *J. Org. Chem.* **1987**, *52,* 4319.
[42] Blum, Y.; Reshef, D.; Shvo, Y. *Tetrahedron Lett.* **1981**, *22,* 1541.
[43] Blum, Y.; Czarkie, D.; Rahamim, Y.; Shvo, Y. *Organometallics* **1985**, *4,*1459.
[44] Zhang, J.; Gandelman, M.; Shimon, L. J. W.; Milstein, D. *Dalton Trans.* **2007**, 107.
[45] Guananathan, C.; Shimon, L. J. W.; Milstein, D. *J. Am. Chem. Soc.* **2009**, *131,* 3146.
[46] Stephan, D. W.; Erker, G. *Angew. Chem. Int. Ed.* **2010**, *49,* 46 .
[47] Berkefelt, A. *J. Am. Chem. Soc.* **2010**, *132,* 10660.
[48] Pierpont, C. G.; Lange, C. W. *Prog*. *Inorg*. *Chem*. **1994**, *41*, 381.
[49] Attia, A. S.; Pierpont, C. G. *Inorg*. *Chem*. **1998**, *37*, 3051.
[50] Dureen, M. A.; Lough, A.; Gilbert, T. M.; Stephan, D. W. *Chem*. *Commun*. **2008**, 4303.
[51] Ung, T.; Hejl, A.; Grubbs, R. H.; Schrodi, Y. *Organometallics* **2004,** *23,* 5399.
[52] Menard, G.; Stephan, D. W. *J*. *Am*. *Chem*. *Soc*. **2011,** *132*, 1796.
[53] (a) Doering, G.; Erker, G.; Froehlich, R.; Meyer, O.; Bergander, K.; *Organometallics* **1998,** *17*, 2183. (b) Cabrera, L.; Welch, G. C.; Masuda, J. D.; Wei, P.; Stephan, D. W. *Science* **2006,** *314*, 1124.
[54] Moemming, C. M.; Otten, E.; Kehr, G.; Froehlich, R.; Grimme, S.; Stephan, D. W.; Erker, G. *Angew. Chem. Int. Ed.* **2009,** *48,* 6643.

[55] Petrucci, R.H.; Herring, G.; Madura, J.D.; Bissonnette, C. *General Chemistry: Principles and Modern Applications*, 10th Edition, Pearson Education, Boston.
[56] Fester, G.W.; Eckstein, J.; Gerlach, D.; Wagler, J.; Brendler, E.; Kroke, E. *Inorg. Chem*. **2010,** *49*, 2667.
[57] Summerscales, O. T.; Myers, T. W.; Berben, L. A. *Organometallics* **2012,** *31*, 3463.
[58] Azhakar, R.; Ghadwal, R. S.; Roesky, H. W.; Hey, J.; Stalke, D. *Dalton Transactions* **2012,** *41*, 1529.
[59] Shipov, A. G.; Korlyukov, A.A.; Kramarova, E.P.; Arkhipov, D.E.; Bylikin, S. Y.; Hunze, F.; Pogozhikh, S. A.; Murasheva, T. P.; V. V. Negrebetskii, V. V.; Khrustalev, V. N.; Ovchinnikov, E.; Bassindale, A. R.; Taylor, P. G. A.; Baukov, Y. I. *Russian Journal of General Chemistry* **2011,** *81,* 2412.

Chapter 2: Metal Ligand Cooperation in ($^{Ph}I_2P^{2-}$)AlH and the Activation of Primary Alcohols

2.1 Introduction

Previously discussed in detail, metal-ligand cooperation has recently been reported as playing an aiding role with catalysis because of the ligands affect on the properties of the metal center. By undergoing reversible structural changes in the process of activating a substrate for formation of the product, the ligand aids in the bond making or bond breaking as part of the catalytic cycle.[1,2]

The addition of an O-H bond across a metal-ligand bond is an innovative alternative to oxidative addition at a metal center. Milstein and coworkers, for example, have reported the activation of water, where a ruthenium hydroxide complex is formed through the O-H bond addition across the ruthenium- ligand bond.[3] Berben and coworkers have also demonstrated the addition of water across metal-ligand bonds utilizing the bis(imino)pyridine ($^{Ph}I_2P^{2-}$) ligand system. The reaction between $^{Ph}I_2PAlH$ ($^{Ph}I_2P$= bis(imino)pyridine) (**1**) and 0.5 equivalents of H_2O yields [($^{Ph}HI_2P^{-}$)AlH(OH)]$_2$(μ-O), by undergoing protonolysis. This complex is capable of reacting further with excess water to yield [($^{Ph}I_2P^{-}$)Al(OH))]$_2$(μ-O), an oxygen and water stable compound.[4]

Figure 2-1. $^{Ph}I_2P$

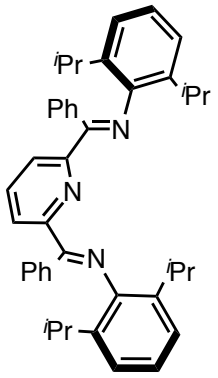

In its 2$^-$ oxidation state, the bis(imino)pyridine ligand system has shown interesting potential in bond activation and catalysis. Myers and Berben recently reported that the bis(imino)pyridine aluminum complex activates N-H bonds via a metal ligand cooperative mechanism where the activation of said N-H bond initates

amine dehydrogenation catalysis and can successfully convert benzylamine into a homocoupled imine.[5]

The bis(imino)pyridine ligand has demonstrated its redox non-innocence in several transition metal complexes. [6,7,8,9,10] Heterolytic bond activation has been reported with group 13 metal centered complexes, including the activation of C-H[11] and N-H bonds,[12] however O-H cleavage has just begun to emerge in the literature.[4] Achieving the O-H activation at an aluminum complex, or beginning the catalytic cycle of dehydrogenation of an alcohol via the aluminum-amido complex, would certainly be a substantial contribution to this area of synthetic chemistry.

Conventionally oxidative addition reactions are precluded by a d^0 electron configuration because it involves the removal of electrons from the metal center, usually requiring a strong electron donor ligand. However, using metal-ligand cooperation, the reducing power of this ligand is harnessed. It is realized that the metal and the ligand react in a cooperative manner to effect the bond-activation reaction. Previously reported by Myers, 4 coordinate aluminum complexes of the formula ($^{Ph}I_2P$)AlX, where X= H, that show examples of amine bond activation via metal-ligand cooperation.[4,5] This chapter will highlight the steps taken in synthesizing the $^{Ph}I_2P$AlH complex and the reactivity with primary alcohols in attempt to create bis(imino)pyridine aluminum-oxo complexes, as well as produce their corresponding aldehydes and H_2.

2.2 Results and Discussion

To continue to investigate this aluminum complex's capabilities, the air sensitive synthesis of ($^{Ph}I_2P$)AlH (**1**) had to be replicated successfully (Scheme 2-1).

Scheme 2-1: Reaction pathway to the aluminum hydride complex **1**.

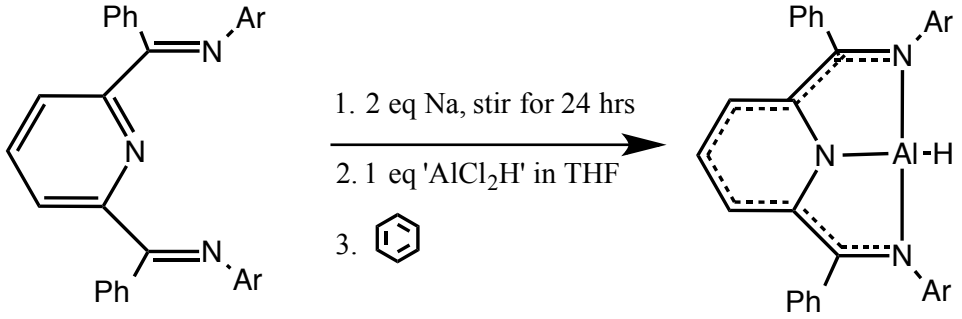

Ar = diisopropylaniline **1**

The ^{1}H-NMR spetrum in Figure 2-2 provides evidence that the aluminum hydride complex can be successfully isolated following the literature methods.[5] Figure 2-3 illustrated the IR spectrum that shows a distinct band at 1781 cm^{-1} indicitive of the Al-H bond stretching vibration. An absorption band at 1592 cm^{-1} and 1628 cm^{-1} are characteristic of the imine C-N stretching vibration (Table 2-1).

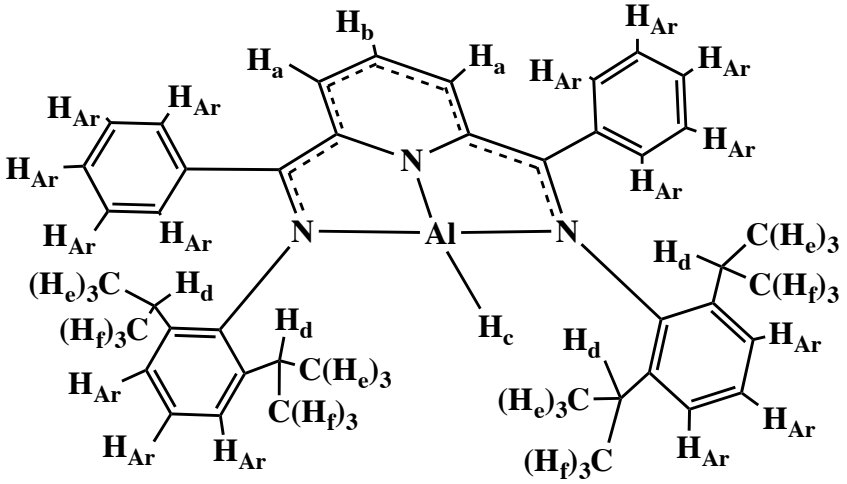

Figure 2-1: Detailed illustration of the Al-H complex **1** to distinguish the different hydrogens.

(b)

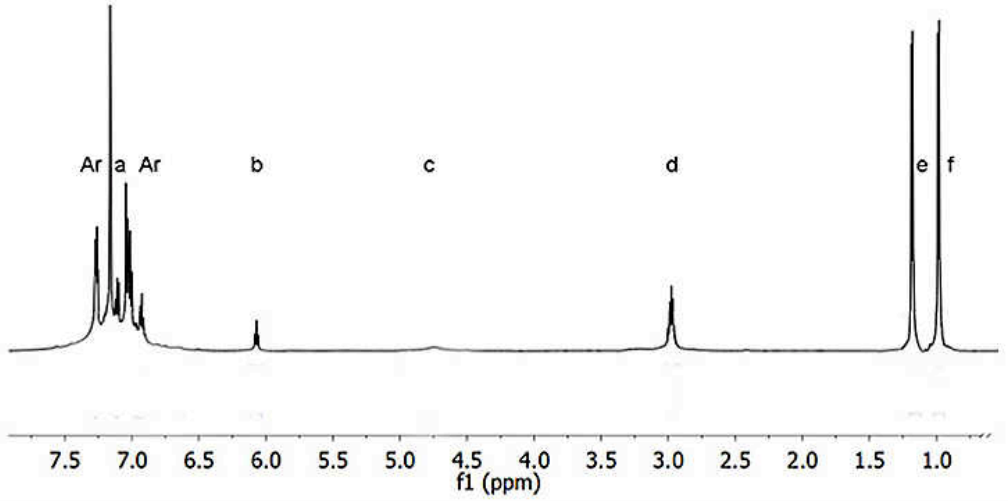

Figure 2-2: ^{1}H NMR spectra of ($^{Ph}I_2P^{2-}$)AlH.

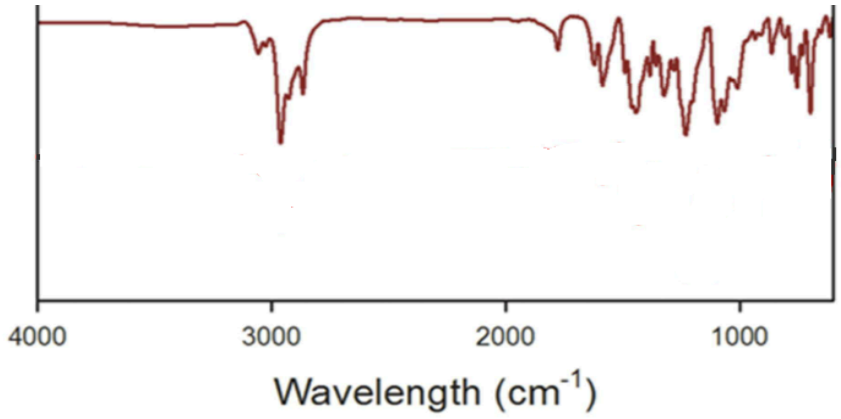

Figure 2-3: The IR spectrum of **1**.

Table 2-1: A table of characteristic absorption bands for **1**.

	C_{im}-N_{im}	**Al-H**	**NH($^{Ph}HI_2P$)**	**NH(ArNH)**
($^{Ph}I_2P^{2-}$)AlH	1592, 1628	1781	N/A	N/A

2.2.1 Activation of Primary Alcohols via $^{Ph}I_2PAlH$ and the Successful Syntheses of $(H^{Ph}I_2P^-)AlH(OC_6H_5)$ and $(H^{Ph}I_2P^-)AlH(OC_4H_9)$

Several different alcohols were used in conjunction with **1** to determine if Al-O bond formation would occur. From previous investigations within the Berben group involving the N-H activation in amines, it was presumed **1** would undergo the same increase in aromaticity within the ligand's pyridine unit, when the amino N-donor ligand is protonated upon bond activation. These changes are easily detected using NMR spectroscopy. Both phenol and ^{t}BuOH were utilized in the attempt to isolate the aluminum alkoxide compound, where the O-H bond of the alcohol is added across the aluminum-amido bond of **1**. Phenol is a suitable reactant because the oxygen is tightly coupled to the aromatic ring. Since phenol has a pKa of 10.02, it can readily undergo proton transfer upon binding to the aluminum (III) center. The initial reaction is simply mixing **1** with a 1 M primary alcohol solution under a N_2 atmosphere. The most challenging aspect of the reaction is the air sensitivity of both the initial hydride complex, as well as the final product.

The 1:1 reaction of **1** and phenol in toluene at room temperature was successful (Scheme 2-1) and $(^{Ph}I_2P^-)AlH(OC_6H_5)$ **(3)** was obtained as a dark blue solution as confirmed by the ^{1}H-NMR spectra. The protonation of the amido N-donor arm on the doubly reduced ligand is a clear, sharp singlet at 6.14 ppm. The aromatized ring of the phenol is difficult to distinguish from the numerous phenyl ring substituents in the range between 6.5 and 7.5 ppm. However, the proton from the O-H group in pure phenol is not present (literature value, 5.30 ppm. Figure 2-4).

Scheme 2-1: Reaction pathway for aluminum phenoxide complex formation.

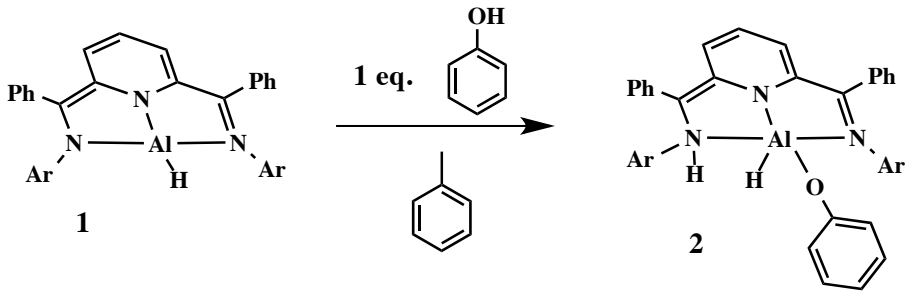

The initial reaction involves simply mixing **1** with a 1 M primary alcohol solution under a N2 atmosphere. The most challenging aspect of the reaction is the air sensitivity of both the initial hydride complex, as well as the final product. Here, the amido-N-donor arm of the $^{Ph}I_2P^{2-}$ ligand is protonated and turns from a yellow to a dark blue color in solution. A similar noteworthy color change from a dark brown solution of **1** to a dark blue was observed after the addition of ^{t}Bu-OH. In the initial reactions, both PhOH and ^{t}Bu-OH were added in 1 molar equivalent amounts in order to isolate the bound substrate. Both solutions began dark brown, but the reaction with PhOH turned dark blue and was isolated, while the reaction with ^{t}Bu-OH turned dark green immediately. From previous work done by Berben and coworkers, the dark green solution obtained during an oxidation reaction with **1** can be recognized as an oxidation of the ligand, not the metal complex. However, the reaction was repeated and replicated to isolate the bound ^{t}BuOH via ^{1}H-NMR spectroscopy. The intermediate blue solutions from the PhOH and ^{t}Bu-OH reactions were obtained at room temperature, purified, and characterized via ^{1}H-NMR in C_6D_6 (Figure 2-3 through 2-6).

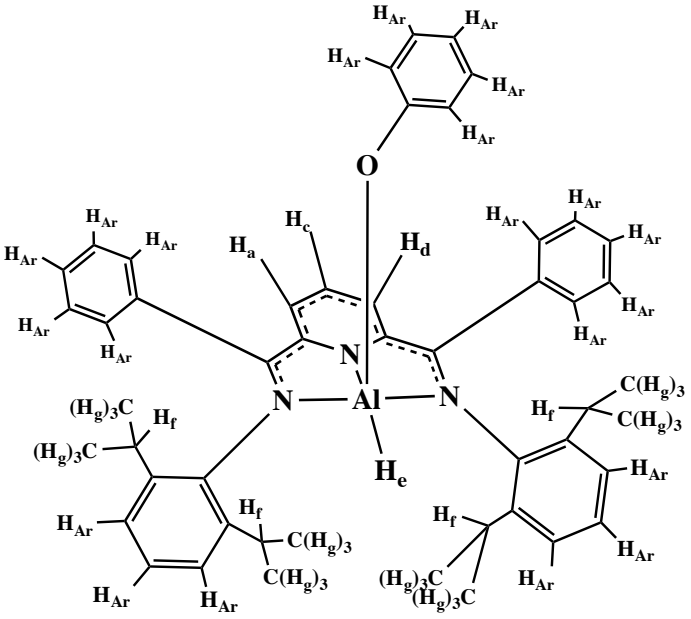

Figure 2-3: Proposed structure of the product of the phenol reaction, with the oxygen is bound to the aluminum atom of **1**.

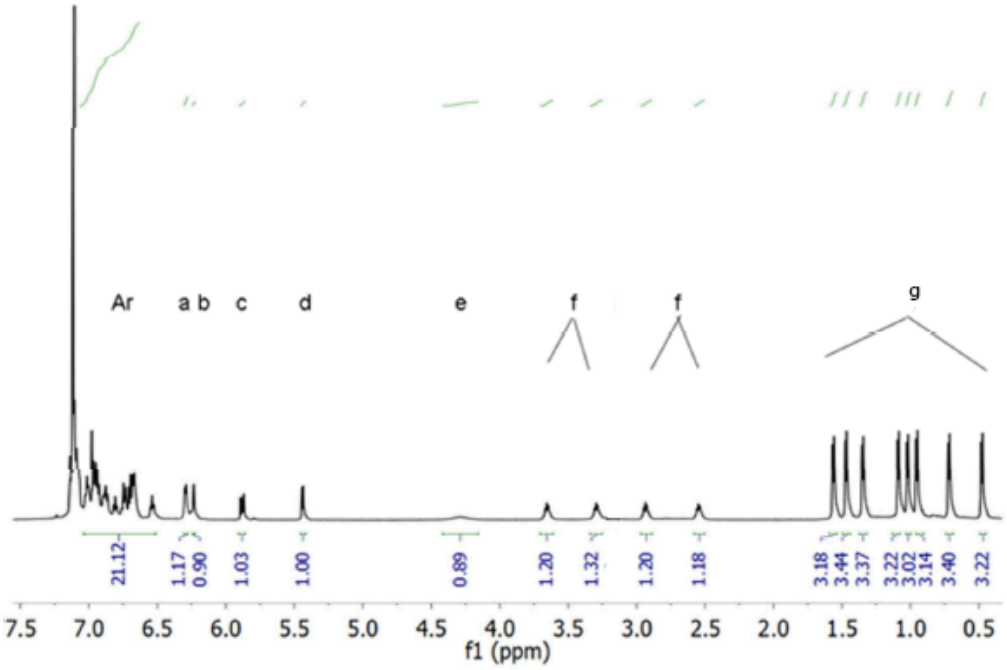

Figure 2-4: ^{1}H-NMR of the blue intermediate of the rection of **1** with PhOH taken in C_6D_6, The fifth bound hydride signal is very broad due to its lability.

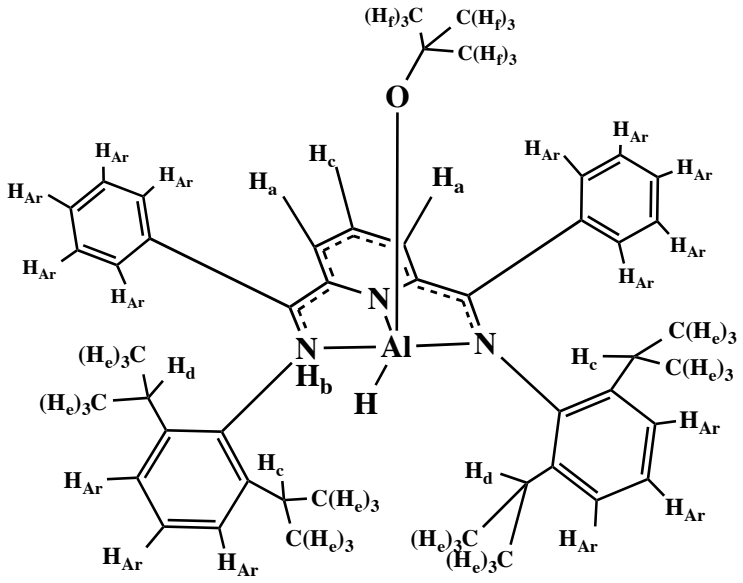

Figure 2-5: Proposed structure of the reaction product of ^{t}Bu-OH, with the oxygen is bound to the aluminum atom of **1**.

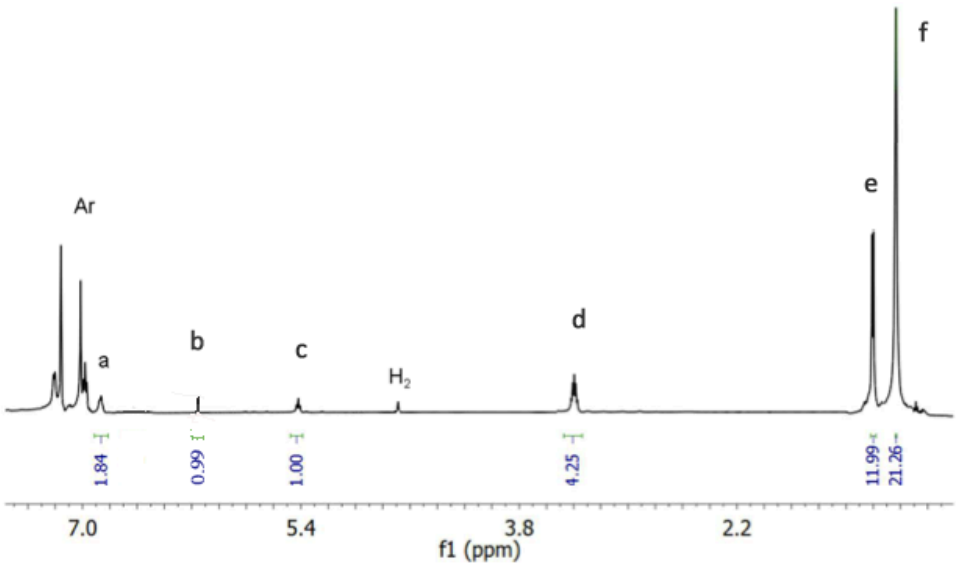

Figure 2-6: ^{1}H-NMR spectrum in C_6D_6 of the reaction of **1** with ^{t}Bu-OH.

The aluminum-oxygen bond is very strong,[7] which in the case of phenol and *tert*-butyl alcohol, denies any kind of catalytic turnover of H_2. Like the recently reported reactivity with water,[5] the ($^{Ph}I_2P^{2-}$)AlH complex reacts with phenol and *tert*-butyl alcohol

for which an activation product is observed (Figure 2-4 and 2-6, respectively), however heating the aluminum oxide products lead to a green solutions indicating decomposition. In contrast to the previously reported reaction with aniline, no H_2 was observed.[5]

2.2.2 Activation of Alcohols containing β Hydrogen and Potential Catalysis

To expand the study of the bond activation to potential dehydrogenation catalysis, alcohols containing *beta*-hydrogen were investigated. Previous reports of activation and dehydrogenation of alcohols via transition metal-ligand cooperative complexes have shown to have a catalytic production of H_2.. Simultaneously, these complexes aid in the transformations of the alcohol into its corresponding aldehyde or ester.[6] The reactions between aldehydes formed in solution were also explored. It was found that a known mechanism for the Tishchenko reaction describes the dimerization of aldehydes to produce esters via a catalytic metal complex, lanthanide alkoxide, or alkali alkoxide.[7] This discovery initiated interest into **1**'s catalytic ability with alcohols and their aldehyde side products, since similar homocoupled reactivity was seen with **1** and benzylamine.[5] This presumes the excess alcohol continuing to react with the catalyst in producing H_2, will also react with the oxygen-bound aldehyde, presumptively coupling and forming an ester. First attempted with benzyl alcohol, Scheme 2-2 depicts the proposed mechanism of the reaction of benzyl alcohol as the primary alcohol with **1**.

Scheme 2-2: Proposed ester formation mechanism employing **1** as a catalyst and benzyl alcohol as the electrophile.

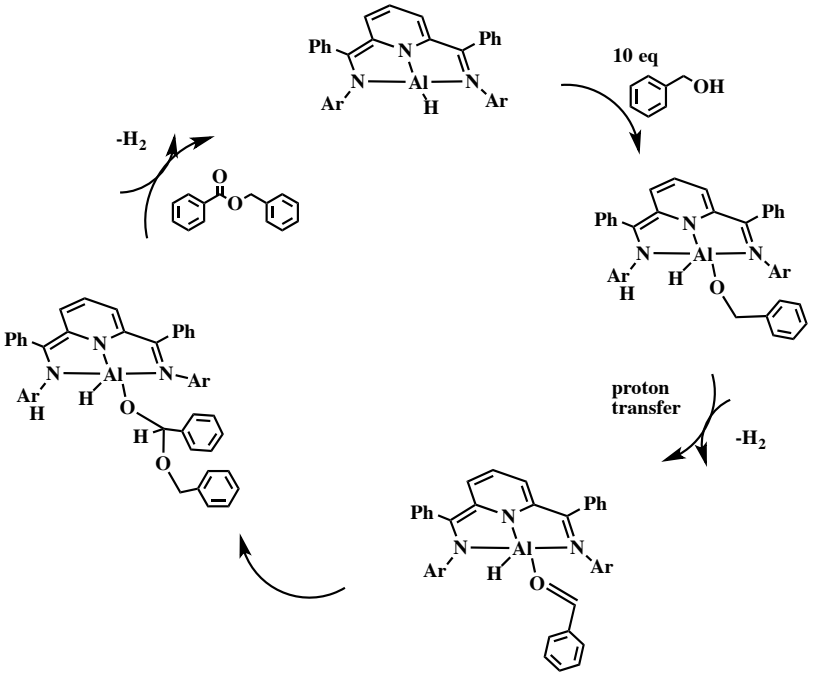

However, it can also be presumed that once bound to the metal, the oxygen bound aldehyde species releases an aldehyde upon releasing H_2 and undergoes proton transfer. Scheme 2-3 depicts the presumed mechanism for such a reaction.

Scheme 2-3 (above): Proposed aldehyde formation mechanism/catalytic cycle of **1** and R-OH.

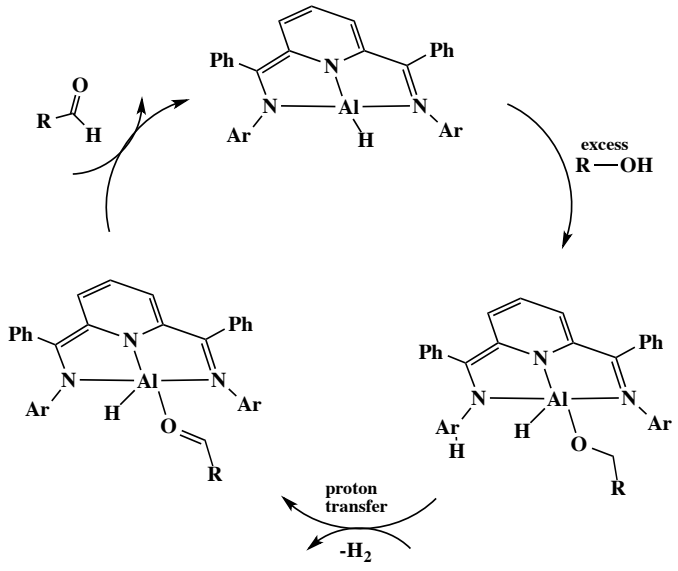

In order to complete either of the above cycles and release H_2 during the reaction of the corresponding aldehyde or ester, the alcohol must have beta hydrogen available for proton transfer. Benzyl alcohol, 1-octanol, and methanol were chosen as reactants with **1**. Both one equivalent and excess amounts of substrate were reacted with the aluminum hydride complex in a Kontes tube in order to allow for the capture of the H_2 gas produced as a byproduct of the catalysis reaction occurring. The headspace of the vessel was sampled to detect if H_2 was successfully being evolved. In both 1 and 20 equivalents reactions, hydrogen gas was detected by GC-TCD using N_2 as a carrier gas. The instrument was calibrated to detect H_2 in the appropriate amounts and was used to determine turnover (in mmoles) of H_2 gas produced in the reaction. The liquid of the reaction was filtered to remove all metallic material and was analyzed via GCMS to detect all organic byproducts.

The reaction with benzyl alcohol yielded the most successful results. The GCMS showed benzaldehyde formation indicating aldehydes are being formed and esters are not. The peak with the retention time 5.31 minutes showed unreacted benzyl alcohol still in reaction. The last peaks eluting past 8 minutes are signals of decomposing ligand (Figure 2-6 (a)). The MS fragment pattern shows the GCMS library confirmation of the C_7H_6O and C_7H_6OH compounds from the reaction (Figure 2-6 (b)).

(a)

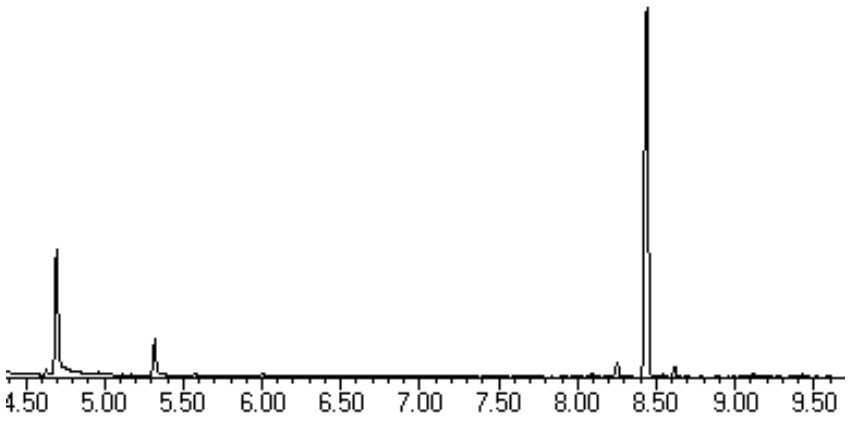

(b)

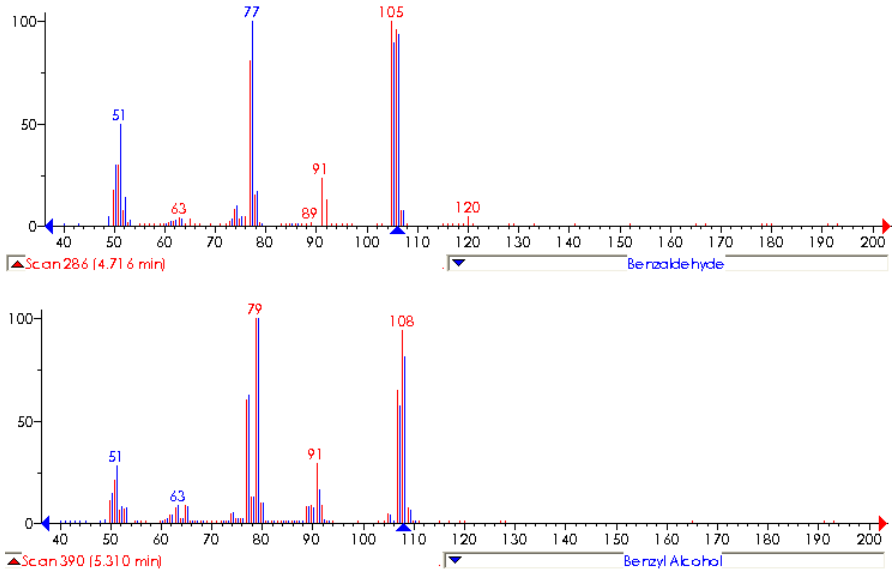

Figure 2-6: (a) The GC analysis of C_7H_6O and C_7H_6OH from the reaction of the **1** complex with benzyl alcohol in toluene.

This provides substantial evidence for the mechanism supporting the formation of an aldehyde from the oxidation of the primary alcohol benzyl alcohol. For secondary evidence, GC measurements were taken of the headspace above the reaction solution for hydrogen gas. These measurements were taken reaction with 20 equivalents alcohol to test for catalytic response from **1**.

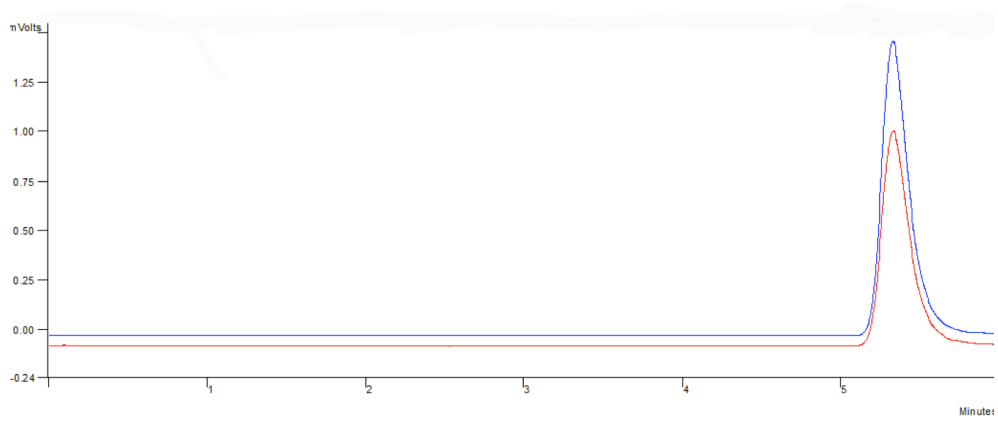

Figure 2-7: GC spectrum of headspace taken of the benzyl alcohol oxidation reaction after being heated and stirred; red shows H_2 formation from 20 equivalents alcohol reaction after 2 minutes after heat application; blue indicates reaction after 24 hours.

Within 2 minutes, the reaction with 20 equivalents benzyl alcohol yielded a turnover number of 1.71, producing 3.34 x 10^{-5} moles of H_2. After 24 hours, the reaction appeared to continue until the aluminum bis(imino)pyridine ligand decomposed. The turnover number (T.O.N.) was calculated to be 2.31, producing 4.62 x 10^{-5} moles of H_2. After 24 hours, the entire reaction used 23% of the substrate to produce H_2 successfully before the ligand system decomposes in solution.

The reaction with 1-octanol proved successful in H_2 production with 20 equivalents alcohol in solution. The T.O.N. was 1.85, producing 3.71 x 10^{-5} moles of H_2. This measurement was taken 2 minutes after heat was applied to the stirring solution. 24 hours after heat was applied, a second measurement was taken of the headspace. The H_2 measurement increased to 6.75 x 10^{-5} moles produced, with a T.O.N. of 3.37. A total of 33% of the substrate had been used in the production of H_2 after 24 hours of reaction time. The GCMS sample did not give any definitive evidence of aldehyde or ester formation from the primary alcohol undergoing an oxidation event. All of the mass

spectrum fragmentation patterns seen were from the solvent and decomposed ligand fragments.

The reaction with methanol gave remarkable results in the production of H_2, showing a production of 4.74 x 10^{-5} moles and a T.O.N. of 2.37, 2 minutes after heat application. After 24 hours, 1.10 x 10^{-4} moles of H_2 were detected with a T.O.N. of 5.55. A total of 55% of the substrate had been used in reaction after 24 hours of reaction time. However, the GC-MS results from the resulting solution of the reaction with 20 equivalents of methanol were skewed. Methanol being such a light molecule makes detection more difficult using GC-MS at a ramped temperature. ^{1}H-NMR was not completely reliable in detecting dimethyl carbonate or any probable organic product forming from the oxidation of methanol. The spectrum taken in C_6D_6 shows several unidentifiable peaks in the up-field region that could account for many unconventional combinations of the methyl alcohol fragments.

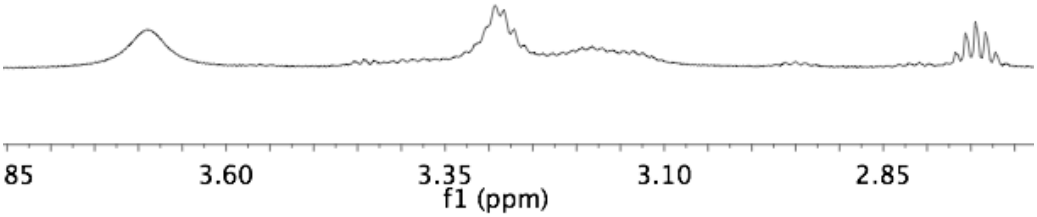

Figure 2-8: The ^{1}H-NMR spectrum in C_6D_6 shows 3 definitive peaks; a broad singlet at 3.69 indicates the formation of dimethyl carbonate.

A broad singlet peak at 3.69 ppm in the ^{1}H-NMR spectrum indicates there could be a formation of the dimethyl carbonate final product. The lack of a peak at 3.07 ppm in the

spectrum shows no residual methanol present in the sample. However, the unidentified peaks nearby, a quintuplet at 2.75 ppm and possible septuplet at 3.29 ppm signify a roughly 1:1:1 ratio of product formation with 2 unknown other major products.

2.3 Conclusions and Avenues for Future Studies:

The ($^{Ph}I_2P^{2-}$)AlH complex has proved viable metal-ligand cooperation in oxidation of the primary alcohol benzyl alcohol. Although full catalytic requirements have yet to be met, the aluminum bis(imino)pyridine hydride complex has shown the ability to bind a primary alcohol and release H_2 successfully. Other primary alcohols such as methanol and 1-octanol have shown the ability to produce H_2 (not quantified), but further investigations are necessary to quantify successfully the H_2 evolved as well as prove their mechanistic routes in catalysis.

Further investigations into substituted benzyl-containing alcohols show great potential to form the corresponding aldehyde in reaction with **1**. Future studies could include investigation into aldehyde and alcohol reactivity to see if hemiacetal or acetal formation occurs. Future catalytic studies could also include repeating similar reactions in a completely air-free system to see if the aldehydes dimerize and form esters. If successful, this aluminum bis(imino)pyridine complex continues to display promise in similar catalytic cycles involving small molecule conversion. These sustainable reactions could also replace more traditional ones that are notorious for their toxic waste product from powerful solvents or reagents, as well as replace costly precious metals with aluminum for large-scale syntheses.

2.4 Experimental Details:

Physical Measurements: ^{1}H NMR spectra were recorded at ambient temperature using a Varian 600 MHz spectrometer. Chemical shifts were referenced to residual solvent. Infra-red (IR) spectra were recorded on a Bruker Tensor Infra-red spectrameter. Quantitative measurement of H_2 was performed on a Varian 3800 GC equipped with a TCD detector with N_2 as a carrier gas; column temperature 100 °C,flow rate: 3mL/min; column details: Supelco Carboxen-1010 PLOT Capillary GC Column (30m x 0.53 mm x 30 μm). H_2 is observable ~5 min and was measured using a calibration curve.

All organic fractions were analyzed by gas chromatography-mass spectroscopy, which was recorded on a GCMS-QP 2010 Shimadzu spectrometer, using helium gas as a carrier at 1.12m mL min^{-1}. The chromatography separation was afforded using a Shimadzu SHRXI-5MS (#0m x 0.25mm x 0.25 μm) and then holding it at 300°C for 25 minutes. The injector temperature was set up to 250°C. On the mass spectrometer, the interface temperature and the ion source temperature were set up to 250 and 200°C respectively.

Preparation of Compounds: All manipulations were carried out using standard Schlenk or glove-box techniques under a dinitrogen atmosphere. Unless otherwise noted, solvents were deoxygenated and dried by thorough sparging with argon gas, followed by passage through an activated alumina column. Deuterated solvents were purchased from Cambridge Isotopes Laboratories, Inc. and were degassed and stored over activated 3 Å molecular sieves prior to use. $^{Ph}I_2P$ was synthesized according to literature methods.[2] All alcohol substrates were purified by fractional distillation[11] and stored over activated 3 Å molecular sieves prior to use. All other reagents were purchased from commercial vendors at HPLC grade and used without further purification.

($^{Ph}I_2P^{2-}$)AlH (1): Solid sodium (46.0 mg, 2.00 mmol) was stirred with $^{Ph}I_2P$ (606 mg, 1.00 mmol) in THF (10 mL) for 24 hours after which the solution was a uniform purple color. Concurrently, $AlCl_3$ (100 mg, 0.75 mmol) was stirred with $LiAlH_4$ (11.4 mg, 0.3 mmol) in THF (10 mL) for 24 hours. The resulting suspension of "$AlCl_2H$" was added slowly to the purple solution of $Na_2(^{Ph}I_2P^{2-})$ at room temperature. The resulting burgundy solution was evaporated to dryness. The solid was dissolved in benzene (20mL) and stirred for 4 hours. The resulting dark brown/bronze solution was dried under vacuum for 24 hours and room temperature. The resulting dark brown solid was obtained in 93% yield. ^{1}H-NMR (600 MHz, C_6D_6): 7.26 (d, J = 7.1, 4H, Ph), 7.13 (d, J = 8.1, 2H, py), 7.05-6.91 (m, 8H, Ar), 6.07 (t, J = 7.5, 1H, py), 4.74 (br, 1H, Al-H), 2.98 (sept, J = 6.9, 4H, C*H*$(CH_3)_2$), 1.18 (d, J = 6.8, 12H, CH(C*H*$_3)_2$), 0.98(d, J = 6.9, 12H, CH(C*H*$_3)_2$) δ IR (KBr): 1781 (m, Al-H), 1628 (im), 1592 (s, im) cm^{-1}.

Reaction of 1 with phenol: ($^{Ph}I_2P^{2-}$)AlH (10.0 mg) was dissolved in toluene (1mL). One equivalent of phenol (1 M solution, in toluene) was added drop-wise at room temperature until the dark brown/bronze solution turned dark blue. The resulting solution was evaporated to dryness at room temperature. The dark blue solid was dissolved in hexane and cooled to - 25° C to recrystallize. ^{1}H-NMR (600 MHz, C_6D_6): ^{1}H NMR(600 MHz, C_6D_6): 6.86-7.21 (m, 21H, Ar and py), 6.56 (t, J = 7.6, 1H, py), 6.24 (s, 1H, N*H*), 3.63 (sept, J = 7.0, 2H, C*H*$(CH_3)_2$), 3.30 (sept, J = 7.2, 2H, C*H*$(CH_3)_2$), 1.37 (d, J = 6.9, 6H, CH(C*H*$_3)_2$), 1.22 (d, J = 6.8, 6H, CH(C*H*$_3)_2$), 1.11 (d, J = 6.8, 6H, CH(C*H*$_3)_2$), 0.88 (d, J = 6.8, 6H, CH(C*H*$_3)_2$).

Reaction of 1 with ^{t}BuOH: ($^{Ph}I_2P^{2-}$)AlH (10.0 mg) was dissolved in toluene (1mL). One equivalent of *t*-butyl alcohol (1 M solution, in toluene) was added drop-wise and stirred at room

temperature until the dark brown/bronze solution turned dark blue. The resulting solution was evaporated to dryness at room temperature. ^{1}H-NMR (600 MHz, C_6D_6): 7.21-6.95 (m, 16H, Ar), 6.86 (d, J = 7.1, 2H, py), 5.65 (br, 1H, NH-$^{Ph}I_2P$), 5.42 (t, J = 7.2, 1H, py), 3.40 (sept, J = 8.0, 4H, CH(CH_3)$_2$), 1.20 (d, J = 7.9, 12H, CH(CH_3)$_2$), 1.03 (m, 21H, ^{t}Bu and CH(CH_3)$_2$) δ.

Reaction of 1 with MeOH: ($^{Ph}I_2P^{2-}$)AlH (10.0 mg) was dissolved in toluene (1mL). 20 equivalents of methanol (1 M solution, in toluene) was added drop-wise and stirred into solution at room temperature. The resulting dark green solution was heated to 70° C to release H_2 . The final solution turned an orange/yellow color. ^{1}H-NMR (600 MHz, C_6D_6): A broad singlet at 3.69 ppm corresponds to dimethyl carbonate in deuterated benzene. Other peaks are unidentified or are decomposed ligand fragments.

Reaction of 1 with benzyl alcohol: ($^{Ph}I_2P^{2-}$)AlH (10.0 mg) was dissolved in toluene (1mL). 20 equivalents of benzyl alcohol (1 M solution, in toluene) was added drop-wise and stirred into solution at room temperature. The resulting dark green solution was heated to 70° C to release H_2. The final solution turned an orange/yellow color. Samples for GCMS were diluted in toluene. Retention time 4.71 minutes = benzaldehyde, 5.31 minutes = residual/unreacted benzyl alcohol.

Reaction of 1 with 1-octanol: ($^{Ph}I_2P^{2-}$)AlH (10.0 mg) was dissolved in toluene (1mL). 20 equivalents of 1-octanol (1 M, in toluene) was added drop-wise and stirred into solution at room temperature. The resulting dark green solution was heated to 70° C to release H_2. The final solution turned an orange/yellow color.

References:

[1] Guananathan, C.; Milstein, D. *Acc. Chem. Res.* **2011,** *44,* 588.
[2] Milstein, D. *Top. Catal.* **2010**, *53,* 915.
[3] Kohl, S.W.; Schwartsburd, L.; Konstantinovski, L; Shimon, L.J.W.; Ben-David, Y.; Iron, M.A.; Milstein, D. *Science* **2009**, *324,* 74.
[4] Myers, T.W.; Berben, L.A. *Organometallics* **2013,** *32,* 6647.
[5] Myers, T.W.; Berben, L.A. *J. Am. Chem. Soc.* **2013**, *135,* 9988.
[6] Zhang, G.; Vasudevan, K. V.; Scott, B. L.; Hanson, S. K. *J. Am. Chem. Soc.* **2013,** *135,* 8668.
[7] Murahashi, S. I.; Naota, T.; Ito, K.; Maeda, Y.; Taki, H. *J. Org. Chem.* **1987**, *52,* 4319.
[8] Milsmann, C.; Turner, Z.R.; Semproni, S.P.; Chirik, P.J. *Angew. Chem. Int. Ed.* **2012**, *51*, 5386.
[9] Cladis, D.P.; Kiermicki, J.J.; Fanwick, P.E.; Bart, S.C. *Chem. Commun.* **2013**, *49*, 4169.
[10] Wieder, N.L.; Gallagher, M.; Carroll, P.J.; Berry, D. H. *J. Am. Chem. Soc.* **2010**, *132*, 4017.
[11] Schöffel, J.; Šušnjar, N.; Nückel, S.; Sieh, D.; Burger, P. *Eur. J. Inorg. Chem.* **2010**, 4911
[12] Fedushkin, I.L.; Skatova, A.A.; Fukin, G.K.; Hummert, M; Schumann, H. *Eur. J. Inorg. Chem.* **2005**, 2332.
[13] Chai, C. L. L.; Armarego, W. L. F. *Purification of Laboratory Chemicals*; 6 ed. Butterworth-Heinemann: Oxford, 2003.

Chapter 3: Synthesis and Characterization of Novel Silicon Complexes

3.1 Introduction:

Areas impacted by the chemistry of frustrated Lewis pairs (FLP) are continuing to grow. While the use of FLPs in stoichiometric[1] and catalytic[2] hydrogenations of imines was the first application to emerge, the development of metal-free hydrogenations[3] continues to intrigue scientists. The evolution of FLPs has resulted in an extensive range of hydrogenation substrates including silylenol ethers[4], enamines[5], enones[6], anilines[7], and heterocycles[8]. Other wonderful development with organometallic substrates[9,10] have been demonstrated in the area of challenging hydrogenations. While aspects and applications of dihydrogen activation continue to be of theoretical and experimental interest, the chemistry of FLPs is certainly not restricted to hydrogen activity. FLPs have been shown to activate a variety of small molecules, including but not limited to, CO_2,[11] B-H bonds,[12] olefins,[13] alkynes,[14,15] and C-H bonds.[16] This wide variety of reactivity foreshadows applications of FLPs in synthetic chemistry. Timely work on greenhouse gas capture and reduction is another provoking area for FLPs to flourish as a part of new strategies in these issues. FLPs are showing interesting and insightful uses in a broadening scope of impact that are brilliant examples of creative new developments that target real world utility.

Investigations in expanding FLP applications into organometallic chemistry are growing rapidly. It was of particular interest to the Berben group to expand on the main group system and look at possibilities with silicon and redox-active ligand systems. Silicon is typically found in 2 oxidation states, 2^+ and 4^+. However the 4^+ is the most common oxidation state and is stable. In exploring alternatives in earth abundant main group

elements, we proposed silicon to be a valuable choice allowing for tuning of electrophilicity or redox potential where applicable.

The coordination of small molecules in generating a six coordinate Si species is well documented[18,19,20,21,] and Si^{4+} metal centers have demonstrated ability to stabilize non-innocent ligands in their reduced states. Examples include $Si(bpy^{2-})_2$[22] and $Si(IP^{2-})(Mes)_2$[24] among several others published between the early 1960's to the present decade.[23,25,26,27,28](bpy = 2-2'-bipyridine, Mes = 2,4,6-trimethylphenyl). A wide variety of challenging synthetic routes to these silicon centered compounds have been reported that include photochemically generated cycloadditions with Si^{2+} intermediates, metatheses of Si^{4+} salts and alkali metals, along with several other methods that result in multiple product formation rather than the desired silicon species.

Silicon used as an organometallic reagent can be challenging due to its capability to access Si^{2+} and Si^{3+} states as well as other undesirable rearrangements. It holds great potential as an alternative Lewis acidic metal center for redox active ligands in the synthesis of novel silicon compounds, as well as developing interest with possible FLP accessibility.

3.2 Results and Discussion

3.2.1 The Catechol Ligand: Past and Present with Silicon Metal Centers

Holmes and coworkers began investigating silicon complexes isoelectronic to phosphoranes. The general features that stabilize the normally high-energy square pyramid for phosphoranes are found to apply equally well to the five-coordinated silicon compounds.[17] Holmes and coworkers reported a successful synthesis of an anionic five-coordinated silicon species with 3,5-ditertbutylcatechol (cat) ligands, with a

tetraethylamine counter cation. This 5-coordinate silicon species has more square pyramidal character in its geometry because of the rigidity of the ring system in the ligands.[17] The bulk of the ligand leaves the last coordination site open for binding, allowing for the production of a neutral silicon complex with the aid of a salt metathesis because of the former ionic nature of the starting material.

This system was used to investigate properties with silicon as the central atom of the complex. The goal was to replicate the Holmes complex from 1985 with the 5th coordination site either bound to easily replaced phenol group or a solvent molecule like tetrahydrofuran (THF). Further FLP type reactivity would be easily explored with a nucleophile with a lower pKa than the solvent or phenol occupying the 5th coordination site on the silicon atom.

3.2.2 Synthesis of $[(cat)_2Si(catH)][Et_3N]$

A variety of silicon starting materials were used based on their solubility and what byproducts or salts they would produce besides the major product. SiR_4 was the starting point for our the desired coordinate complex with two 3,5-di-*tert*-butylcatechol ligands (where R = Cl, Ph-OEt, or Ph-OMe). The byproducts were removed by filtration using celite or by manipulation of their solubility versus the major product.

Scheme 3-1: Proposed reaction scheme for the synthesis of $PhSi(cat)_2$.

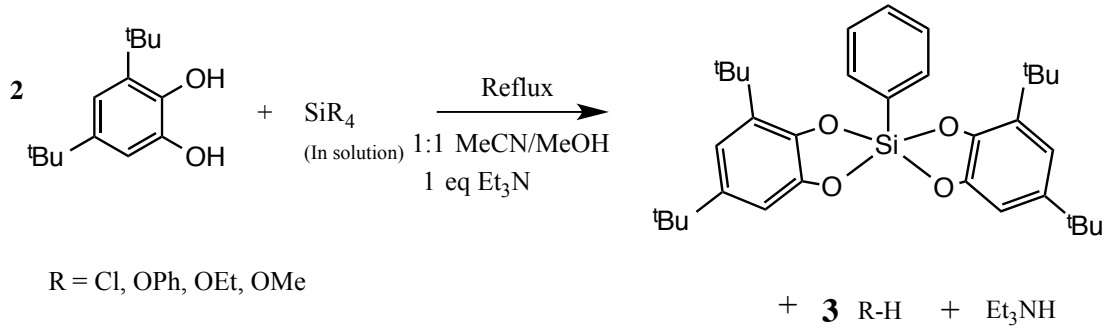

A successful synthesis utilizing $SiCl_4$ gave a single crystal after recrystallization The X-ray crystal structure was determined and differed from the projected product (Figure 3-1 below).

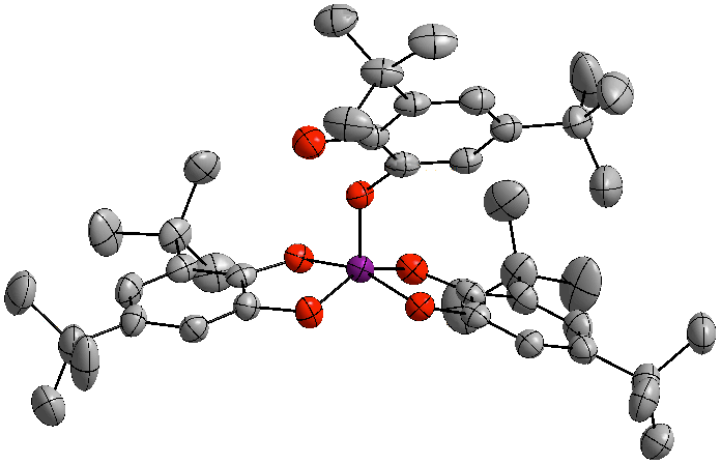

Figure 3-1: Solid state structure of $[(cat)_2Si(catH)][Et_3N]$ (**2**); The triethylamine counter-cation is omitted for optimal visualization of the silicon centered complex.

Table 3-1: Crystallographic data for **2**

Crystal Size	0.205 x 0.298 x 0.381
Formula weight, g mol^{-1}	1024.25
a, Å	8.6951
b, Å	29.0176
c, Å	11.0681
α, degree	90.000
β, degree	106.793
γ, degree	90.000
V, $Å^3$	2670.44
Z	2
T, K	190.15
ρ, calcd, g cm^{-3}	1.274
Refl. Collected/$2\theta_{max}$	16904/140.16
Unique refl./ $I>2\sigma(I)$	4884
No. parameters/restrains	525/2
λ, Å/μ(Kα), cm^{-1}	1.54178
R1/GOF	0.0706/2.034
wR2 ($I>2\sigma(I)$)	0.1922
Residual density, e $Å^{-3}$	0.10
Space Group	P2(1)
Formula	$SiC_{46}O_6H_{76}N$

Table 3-2: Noteworthy average bond lengths (Å) and angles for **2**

	Avg Angle (degree)	Avg Bond Length (Å)
Si-O_1		1.7551
Si-O_2		1.7221
Si-O_3		1.7192
Si-O_4		1.7099
Si-O_5		1.6815
Si-O_1-C	113.15	
Si-O_2-C	112.02	
Si-O_3-C	114.86	
Si-O_4-C	112.87	
Si-O_5-C	131.22	

The structure determined showed a third 3,5-di-*tert*-butylcatechol ligand is bound to the silicon metal center in the 5th coordinate site. At first sight, the stoichiometry of the reaction would appear to be 1:3 instead of the appropriate 1:2 ratio. However, when $SiCl_4$ is added to the solution, HCl gas is formed rapidly as a byproduct. It is believed that the entire equivalent of $SiCl_4$ does not get fully dissolved into solution, therefore more ligand would be available in solution then the subsequent silicon starting material in order to have only 2 ligands bind to the central silicon atom.

While analyzing the crystallographic data for the compound, it was found that one of the Si-O bond lengths are substantially shorter. This is due to the one oxygen from the third ligand (O_5) being bound to the central atom's 5th coordination site and the sixth oxygen not being bound to the central silicon atom, but to a hydrogen. Since these were the first successful silicon catechol product, our next step was to use this complex and isolate the desired complex by exchanging out the 5th ligand. The first attempts used salt metathesis in order to try and drive the reaction by producing a salt byproduct.

Using 1 eq. NaOMe, in reaction with 2, it was proposed that the methoxy group would replace the bound catechol and the sodium catechol salt would form. The structure obtained was the desired product from using the $Si(OMe)_3$ starting material as well. A bulkier Bu_4N^+ counter cation was used in simultaneous syntheses utilizing the Bu_4NI salt. Other efforts were made utilizing $[HB[3,5\text{-}(CF_3)_2C_6H_3]_4]$, or the protonated form of the so-called BAr^F non-coordinating anion, to create a neutral compound with a THF solvent molecule possibly bound in the 5th coordinate site. All reactions first began

with dissolving the SiR_4 starting material into a small amount (~5 mL) of solvent and then titrating the solution into the larger ligand solution while stirring. All attempts proved unsuccessful in obtaining the desired silicon catechol product. The silicon oxygen bond is extremely strong having both covalent and ionic character, so it is assumed the energy necessary to break the Si-O bond was not met by any of these reaction series.

Therefore, complex **2** was unique it its synthesis and characterization, but did not qualify for further FLP chemistry, given the 5th coordination site is occupied by a third catechol ligand that does not have the FLP character necessary to carry on reactivity series testing the capability of reducing small molecules.

3.3 Investigating Variations in the Ligand System with Silicon: The 2,4-di-*tert*-butyl-6-*tert*butylaminophenol (apH_2) ligand became of interest when the 3,5-di-*tert*-butylcatechol ligand didn't seem to have enough steric bulk to keep a third catechol ligand from binding to the silicon's open 5th coordination site.[18] The chelating ligand has an advantage in it's more stericly hindering *tert*-butylamide groups in cis-coordination sites, while the oxygen atoms are in the trans-coordination sites. Heyduk and coworkers

investigated the transition metal complexes utilizing Zn to mimic standard oxidative addition capabilities of a complex with two vacant coordination sites, an electron poor metal center, and metal ion with readily accessible oxidation states (M^{n+} and $M^{(N+2)+}$). This sparked an investigation with the silicon center using the apH_2 ligand to create a redox based bond activation pathway. The amide is a strong base and good nucleophilic candidate to try and create a 4-coordinate silicon complex for further FLP-type reactivity.

The 2,4-di-*tert*-butyl-6-*tert*butylaminophenol ligand was successfully synthesized on a small scale with a 60% yield. A dark green oily product was obtained from a 1:1 mixture of 3,5-di-*tert*-butylcatechol and *tert*-butylamide in acetonitrile. In a glove box, the oily residue was recrystallized from a 1:3 acetonitrile/ ether solvent mixture.

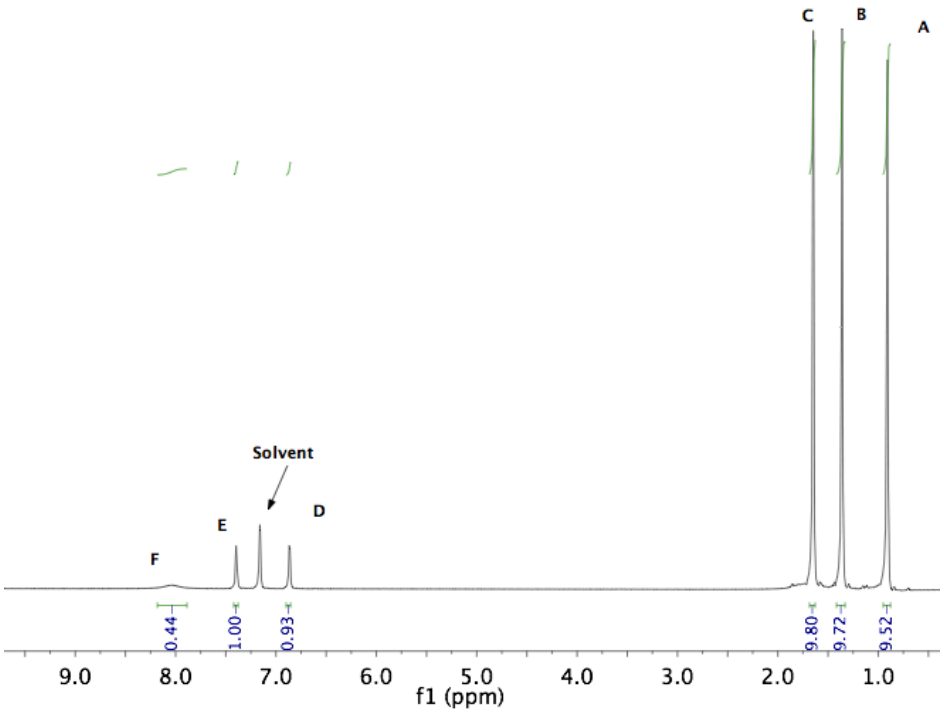

Figure 3-2: ^{1}H-NMR of the 2,4-di-*tert*-butyl-6-*tert*-butylphenol (apH_2) in d_6-benzene.

In a scaled up reaction series however, the product was not successfully obtained. Solvent impurities were negated as the cause for the reaction failure from individual ^{1}H-NMR spectral scans of all starting materials and solvents (A and B). However, in stoichiometric scaled up reactions, the stoichiometry in the reaction flask varies with time and the amount of product and byproduct (C and D) formed will depend on the ratio of A and B starting materials in the vessel at one time. This depends on rate of addition, rate of reaction between the starting materials (varies with temperature, concentration, presence of catalysts, etc.) and especially the mixing in the vessel. Ultimately kinetics of the reaction prevented the large-scale reaction from yielding a substantial amount of major product in order to move onto large-scale metallations and further reactivity investigations.

3.4 Conclusions and Future Direction:

Attempts to metallate the pure batches of the apH_2 ligand with silicon proved unsuccessful. As seen in many cases in the past, multiple products are obtained due to the harsh conditions within the reaction, as well as the propensity of the conjugation within the ligand to radical or electrophilic attack from the reduced silicon species. Complicated results have been reported when using $SiCl_4$ as an organometallic reagent. This was observed in reaction with both the catH_2 and apH_2 ligands. Both $PhSi(OMe)_3$ and $PhSi(OEt)_3$ were also used as 1 equivalent organometallic reagents with the notion that the silicon center would keep the phenyl ring in its 5th coordination site after binding to the bidentate ligand.

Although these attempts were unsuccessful, further investigation into similar ligand systems with milder silicon reagents contains potential for FLP chemistry. Other

abundant main group elements such as Al^{3+} and Mg^{2+} have been shown to complex with redox active ligands, however, less has been reported on FLP reactivity.

3. Experimental Details:

Physical Measurements: ^{1}H NMR spectra were recorded at ambient temperature using a Varian 600 MHz spectrometer. Chemical shifts were referenced to residual solvent.

X-ray Structure determinations: X-ray diffraction studies were carried out on a Bruker SMART 1000, a Bruker SMART APEXII, and a Bruker SMART APEX Duo diffractometer equipped with a CCD detector.[29a] Measurements were carried out at -175 °C using Mo Kα (0.71073 Å) and Cu Kα (1.5418 Å) radiation. Crystals were mounted on a glass capillary or Kaptan Loop with Paratone-N oil. Initial lattice parameters were obtained from a least-squares analysis of more than 100 centered reflections; these parameters were later refined against all data. Data were integrated and corrected for Lorentz polarization effects using SAINT1b and were corrected for absorption effects using SADABS2.3.[29b]

Space group assignments were based upon systematic absences, E statistics, and successful refinement of the structures. Structures were solved by direct methods with the aid of successive difference Fourier maps and were refined against all data using the SHELXTL 5.0 software package.[29c] Thermal parameters for all non-hydrogen atoms were refined anisotropically. Hydrogen atoms, where added, were assigned to ideal positions and refined using a riding model with an isotropic thermal parameter 1.2 times that of the attached carbon atom (1.5 times for methyl hydrogens).

Preparation of Compounds: All manipulations were carried out using standard Schlenk or glove-box techniques under a dinitrogen atmosphere. Unless otherwise noted, solvents were deoxygenated and dried by thorough sparging with Ar gas followed by passage through an activated alumina column. Deuterated solvents were purchased from Cambridge Isotopes Laboratories, Inc. and were degassed and stored over activated 3 Å molecular sieves prior to use. All silicon containing starting materials were purified and stored over activated 3 Å molecular sieves prior to use. All other reagents were purchased from commercial vendors at HPLC grade and used without further purification.

$[(cat)_2Si(catH)][Et_3N]$ (1): 10 mmol (2.22g) of 3,5-di-tert-butylcatechol stirred in 50 mL of MeCN and 30 mL of MeOH while being degassed with N_2 for 15 minutes prior to the addition of the metal or triethylamine. While the flask is submerged in an acetone/ice cooling bath, 5 mmol (0.57mL) of distilled $SiCl_4$ was added to the solution. Excess (~25 mmol) Et_3N was added turning the entire solution a slight yellow color. The solution was then refluxed for 12 hours at 70° C. The resulting solution was evaporated via vacuum and redissolved into hexane and filtered through celite to remove salts. The hexane was evaporated and was recrystallized in a 1:3 MeCN and Et_2O solution and yielded a white solid in low yield (42%). Neither ^{1}H-NMR nor ^{29}Si- NMR conclusive for the complex. Crystallographic data is tabulated above (Table 3-1).

2,4-di-*tert*-butyl-6-(*tert*-butylamino)phenol (apH_2) (2): Prepared by a reported procedure.[30] 3,5-di-tert-butylcatechol 45.0mmol, (10g) was dissolved in 60 mL of acetonitrile. The solution was placed over 3 Å molecular sieves and 4.72 mL (1eq.) of *tert*-butyl amine was added. The solution was refluxed for 2 hours. The solution color changed from pale yellow to dark green. The reaction mixture was filtered and the

sieves were washed with 200 ml of diethyl ether. While under a flow of N_2, the organic layers were combined via cannula into a clean, dry 500 mL flask and washed with a saturated solution of sodium dithionite until the organic layer turned yellow. The organic layer was separated and dried over magnesium sulfate and condensed into an oily residue. In a glove box under N_2, the residue was recrystallized from acetonitrile as a white solid at 62% yeild. ^{1}H NMR (500 MHz, C_6D_6) δ/ppm: 0.90 (s, 9H, N-C(C*H*$_3$)$_3$), 1.35 (s, 9H, Ar-C(C*H*$_3$)$_3$), 1.63 (s, 9H, Ar-C(C*H*$_3$)$_3$), 6.85 (d, 1H, Ar-*H*, $^3J_{HH}$ = 3.00), 7.38 (d, 1H, Ar-*H*, $^3J_{HH}$ = 3.00), 8.01 (s, 1H, N*H*).

References:

1. Heiden, Z. M.; Stephan, D. W. *Chem*. *Comm*. **2011**, *47*, 5729.
2. Stephan, D. W.; Greenberg, S.; Graham, T. W.; Chase, P.; Hastre, J. J.; Geier, S. J.; Farrell, J. M.; Brown, C. C.; Heiden, Z. M.; Welch, G. C.; Ullrich, M. *Inorg*. *Chem*. **2011**, *50*, 12338.
3. Stephan, D. W.; Erker, G. *Angew*. *Chem*. *Int*. *Ed*. **2010**, *49*, 46.
4. Wang, H.; Froehlich, R.; Kehr, G.; Erker, G. *Chem*. *Comm*. **2008**, *45*, 5966.
5. Spies, P.; Scwendermann, S.; Lange, S.; Kehr, G.; Froehlich, R.; Erker, G. *Angew*. *Chem*. *Int*. *Ed*. **2008**, *47*, 7543.
6. Greb, L.; Ona-Burgos, P.; Kubas, A.; Falk, F.C.; Breher, F.; Fink, K.; Paradies, J. *Dalton Trans*. **2012**, *41*, 9056.
7. Mahdi, T.; Heiden Z.M.; Grimme, S.; Stephan, D. W. *J*. *Am*. *Chem*. *Soc*. **2012**, *134*, 4088.
8. Yalpani, M.; Lunow, T.; Koester, R. *Chem*. *Ber*. **1989**, *122*, 687.
9. Axenow, K. V.; Kehr, G.; Froehlich, R.; Erker, G. *Organometallics* **2009**, *28*, 5148.
10. Axenow, K. V.; Kehr, G.; Froehlich, R.; Erker, G. *J*. *Am*. *Chem*. *Soc*. **2009**, *131*, 3454.
11. Xu, X.; Kehr, G.; Daniliuc, C. G.; Erker, G. *J*. *Am*. *Chem*. *Soc*. **2013**, *135*, 6465.
12. DeWitt, E. J.; Ramp, F. L.; Trapasso, L. E. *J*. *Am*. *Chem*. *Soc*. **1961**, *83*, 4672.
13. Osborn, J. A.; Jardine, F. H.; Young, J. F.; Wilkinson, G. *J*. *Chem*. *Soc*. *A*. **1996**, *12*, 1711.
14. Chen, C.; Eweiner, F.; Wibbeling, B.; Froehlich, R.; Senda, S.; Ohki, Y.; Tatsumi, K.; Grimme, S.; Kehr, G.; Erker, G. *Chem*. *Asian J*. **2010**, *5*, 2199.
15. Chen, C.; Kehr, G.; Froehlich, R.; Erker, G. *J*. *Am*. *Chem*. *Soc*. **2010**, *132*, 13594.

16. Menard, G.; Hatnean, J.A.; Cowley, H. J.; Lough, A.J.; Rawson, J.M.; Stephan, D.W. *J*. *Am*. *Chem*. *Soc*. **2013**, *135*, 6446.
17. Holmes, R. H.; Day, R. O.; Chandrasekhar, V.; Holmes, J. M. *Inorg*. *Chem*.**1985**, *24*, 2009.
18. Seiler, O.; Bertermann, R.; Buggisch, N.; Burschka, C.; Penka, M.; Tebbe, D.; Tacke, R.Z. *Anorg*. *Allg*. *Chem*. **2003,** *629*, 1403.
19. Fleischer, H. *Euro*. *J*. *Inorg*. *Chem*. **2001,** 393.
20. Fester, G.W.; Eckstein, J.; Gerlach, D.; Wagler, J.; Brendler, E.; Kroke, E. *Inorg*. *Chem*. **2010,** *49*, 2667.
21. Summerscales, O. T.; Myers, T. W.; Berben, L. A. *Organometallics* **2012,** *31*, 3463.
22. Morancho, R.; Pouvreau, P.; Constant, G.; Joud, J.; Galy, J. *J*. *Organomet*. *Chem*. **1979,** *166*, 329.
23. Herzog, S.; Krebs, F. *Naturwissenschaften* **1963,** *50*, 300.
24. Weidenbruch, M.; Piel, H.; Peters, K.; von Schnering, H.G. *Organometallics* **1993,** *12*, 2881.
25. Haaf, M.; Schmiedl, A.; Schmedake, T.A.; Powell, D.R.; Millevolte, A.J.; Denk, M.; West, R. *J*. *Am*. *Chem*. *Soc*. **1998,** *120*, 12714.
26. Weidenbruch, M.; Piel, H.; Peters, K.; von Schnering, H.G. *Organometallics* **2010,** *13*, 3990.
27. Weidenbruch, M.; Piel, H.; Lesch, A.; Peters, K.; von Schnering, H.G. *J*. *Organomet*. *Chem*. **1993,** *454*, 35.
28. Fester, G. W.; Eckstein, J.; Gerlach, D.; Wagler, J.; Brendlr, E.; Kroke, E. *Inorg*. *Chem*. **2010,** *49*, 2667.
29. (a) SMART Software Users Guide, Version 5.1 Bruker Analytical X-ray Systems, Inc.; (b) Sheldrick, G. M. SADAS, Version 2.03, Bruker Analytical X-ray Sytems, Inc.; Madison, WI 2000. (c) Sheldrick, G. M. SHELXTL Version 6.12, Bruker Analytical X-ray Systems, Inc.; Madison, WI 1999.
30. Blackmore, K. J.; Ziller, J. W.; Heyduk, A. F. *Inorg. Chem.* **2005,** *44,* 5559.

Appendix A

checkCIF/PLATON report

Structure factors have been supplied for datablock(s) mm1-sr for the compound $[(cat)_2Si(catH)][Et_3N]$. Level A alerts due to an accessible solvent void. This void is due to the removal of a disordered THF by a squeeze command in Planton. Level B alerts due to low density. Both alerts are addressed in the following report.

Datablock: mm1-sr

No syntax errors found. CIF dictionary Interpreting this report

---

```
Bond precision:  C-C = 0.0060 A          Wavelength=1.54178

Cell:            a=8.6851(3)    b=29.0176(8)        c=11.0681(3)
                 alpha=90       beta=106.793(1)     gamma=90
Temperature:     90 K
```

	Calculated	Reported
Volume	2670.44(14)	2670.44(14)
Space group	P 21	P2(1)
Hall group	P 2yb	?
Moiety formula	C42 H60 O6 Si	?
Sum formula	C42 H60 O6 Si	C42 H60 Cl0 N0 O6 Si
Mr	688.99	688.99
Dx,g cm-3	0.857	0.857
Z	2	2
Mu (mm-1)	0.645	0.645
F000	748.0	748.0
F000'	750.54	
h,k,lmax	10,35,13	10,35,13
Nref	10181[5198]	8281
Tmin,Tmax	0.793,0.879	0.791,0.879
Tmin'	0.783	

```
Correction method= NUMERICAL

Data completeness= 1.59/0.81      Theta(max)= 70.080

R(reflections)= 0.0706( 7932)     wR2(reflections)= 0.1922( 8281)

S = 1.050                 Npar= Npar = 443
```

The following ALERTS were generated. Each ALERT has the format
test-name_ALERT_alert-type_alert-level.
Click on the hyperlinks for more details of the test.

Alert level A

```
PLAT602_ALERT_2_A VERY LARGE Solvent Accessible VOID(S) in Structure       ! Info
```

Alert level B

```
PLAT049_ALERT_1_B Calculated Density less than 1.0 gcm-3 .........     0.8569
```

Alert level C

```
CRYSC01_ALERT_1_C No recognised colour has been given for crystal colour.
PLAT029_ALERT_3_C _diffrn_measured_fraction_theta_full Low .......      0.960 Note
PLAT041_ALERT_1_C Calc. and Reported SumFormula    Strings  Differ     Please Check
PLAT220_ALERT_2_C Large Non-Solvent  C     Ueq(max)/Ueq(min) Range       3.5 Ratio
PLAT230_ALERT_2_C Hirshfeld Test Diff for    C33    --  C52     ..        5.2 su
PLAT234_ALERT_4_C Large Hirshfeld Difference C33    --  C53     ..       0.17 Ang.
PLAT242_ALERT_2_C Low       Ueq as Compared to Neighbors for .....        C33 Check
PLAT242_ALERT_2_C Low       Ueq as Compared to Neighbors for .....        C49 Check
PLAT309_ALERT_2_C Single Bonded Oxygen (C-O > 1.3 Ang) ...........         O6 Check
PLAT340_ALERT_3_C Low Bond Precision on  C-C Bonds ...............    0.0060 Ang.
PLAT911_ALERT_3_C Missing # FCF Refl Between THmin & STh/L=  0.600       254 Why ?
PLAT915_ALERT_3_C Low Friedel Pair Coverage ......................        68 %
```

Alert level G

```
CELLZ01_ALERT_1_G Difference between formula and atom_site contents detected.
CELLZ01_ALERT_1_G ALERT: Large difference may be due to a
           symmetry error - see SYMMG tests
          From the CIF: _cell_formula_units_Z    2
          From the CIF: _chemical_formula_sum  C42 H60 Cl0 N0 O6 Si
          TEST: Compare cell contents of formula and atom_site data

          atom    Z*formula  cif sites diff
          C         84.00     84.00    0.00
          H        120.00    120.00    0.00
          Cl         2.00      0.00    2.00
          N          2.00      0.00    2.00
          O         12.00     12.00    0.00
          Si         2.00      2.00    0.00
PLAT005_ALERT_5_G No _iucr_refine_instructions_details  in the CIF     Please Do !
PLAT033_ALERT_4_G Flack x Value Deviates > 2*sigma from Zero .....      0.150
PLAT066_ALERT_1_G Predicted and Reported Tmin&Tmax Range Identical          ? Check
PLAT072_ALERT_2_G SHELXL First  Parameter in WGHT Unusually Large.       0.12 Why ?
PLAT912_ALERT_4_G Missing # of FCF Reflections Above STh/L=  0.600        61 Note
PLAT961_ALERT_5_G Dataset Contains no Negative Intensities .......     Please Check
```

```
   1 ALERT level A = Most likely a serious problem - resolve or explain
   1 ALERT level B = A potentially serious problem, consider carefully
  12 ALERT level C = Check. Ensure it is not caused by an omission or oversight
   8 ALERT level G = General information/check it is not something unexpected

   6 ALERT type 1 CIF construction/syntax error, inconsistent or missing data
   7 ALERT type 2 Indicator that the structure model may be wrong or deficient
   4 ALERT type 3 Indicator that the structure quality may be low
   3 ALERT type 4 Improvement, methodology, query or suggestion
   2 ALERT type 5 Informative message, check
```

Datablock mm1-sr - ellipsoid plot

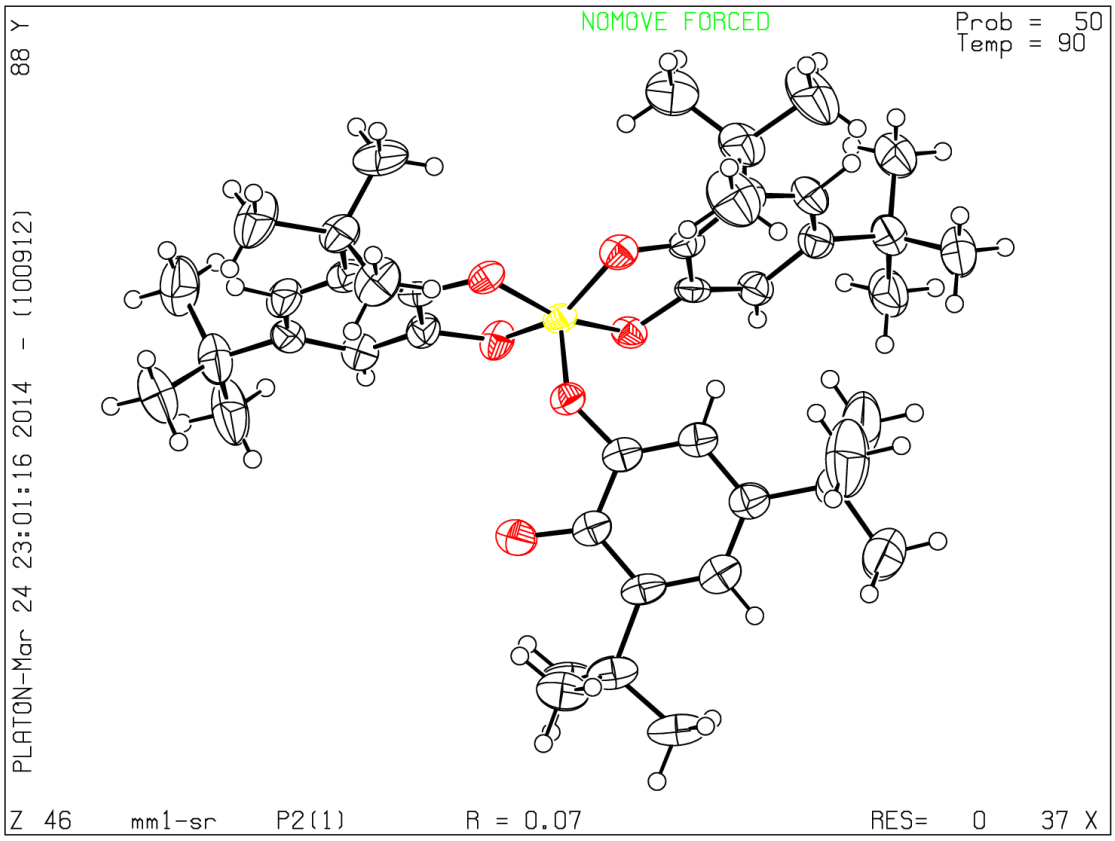

Appendix B

```
CIF File

data_mm1-sr

_audit_creation_method            SHELXL-97
_chemical_name_systematic
;
 ?
;
_chemical_name_common             ?
_chemical_melting_point           ?
_chemical_formula_moiety          ?
_chemical_formula_sum
 'C42 H60 Cl0 N0 O6 Si'
_chemical_formula_weight          688.99

loop_
 _atom_type_symbol
 _atom_type_description
 _atom_type_scat_dispersion_real
 _atom_type_scat_dispersion_imag
 _atom_type_scat_source
 'C'  'C'   0.0181   0.0091
 'International Tables Vol C Tables 4.2.6.8 and 6.1.1.4'
 'H'  'H'   0.0000   0.0000
 'International Tables Vol C Tables 4.2.6.8 and 6.1.1.4'
 'N'  'N'   0.0311   0.0180
 'International Tables Vol C Tables 4.2.6.8 and 6.1.1.4'
 'Si'  'Si'   0.2541   0.3302
 'International Tables Vol C Tables 4.2.6.8 and 6.1.1.4'
 'Cl'  'Cl'   0.3639   0.7018
 'International Tables Vol C Tables 4.2.6.8 and 6.1.1.4'
 'O'  'O'   0.0492   0.0322
 'International Tables Vol C Tables 4.2.6.8 and 6.1.1.4'

_symmetry_cell_setting            monoclinic
_symmetry_space_group_name_H-M    P2(1)

loop_
 _symmetry_equiv_pos_as_xyz
 'x, y, z'
 '-x, y+1/2, -z'

_cell_length_a                    8.6851(3)
_cell_length_b                    29.0176(8)
_cell_length_c                    11.0681(3)
_cell_angle_alpha                 90.00
_cell_angle_beta                  106.7930(10)
```

```
_cell_angle_gamma                  90.00
_cell_volume                       2670.44(14)
_cell_formula_units_Z              2
_cell_measurement_temperature      90(2)
_cell_measurement_reflns_used      100
_cell_measurement_theta_min        2.48
_cell_measurement_theta_max        28.84

_exptl_crystal_description         block
_exptl_crystal_colour              clear
_exptl_crystal_size_max            0.38
_exptl_crystal_size_mid            0.30
_exptl_crystal_size_min            0.20
_exptl_crystal_density_meas        ?
_exptl_crystal_density_diffrn      0.857
_exptl_crystal_density_method      'not measured'
_exptl_crystal_F_000               748
_exptl_absorpt_coefficient_mu      0.645
_exptl_absorpt_correction_type     'numerical'
_exptl_absorpt_correction_T_min    0.7912
_exptl_absorpt_correction_T_max    0.8792
_exptl_absorpt_process_details     'SADABS'

_exptl_special_details;

Squeeze command used to remove a disordered THF and disorderd NEt3
molecule from the unit cell. Hence the Level A alert for accessible
solvent void and the level B error for low measured density.

_diffrn_ambient_temperature        90(2)
_diffrn_radiation_wavelength       1.54178
_diffrn_radiation_type             CuK\a
_diffrn_radiation_source           'fine-focus sealed tube'
_diffrn_radiation_monochromator    graphite
_diffrn_measurement_device_type    'CCD area detector'
_diffrn_measurement_method         'phi and omega scans'
_diffrn_detector_area_resol_mean   ?
_diffrn_reflns_number              16861
_diffrn_reflns_av_R_equivalents    0.0445
_diffrn_reflns_av_sigmaI/netI      0.0603
_diffrn_reflns_limit_h_min         -8
_diffrn_reflns_limit_h_max         10
_diffrn_reflns_limit_k_min         -35
_diffrn_reflns_limit_k_max         34
_diffrn_reflns_limit_l_min         -13
_diffrn_reflns_limit_l_max         12
_diffrn_reflns_theta_min           3.05
_diffrn_reflns_theta_max           70.08
_reflns_number_total               8281
_reflns_number_gt                  7932
_reflns_threshold_expression       >2sigma(I)
```

```
_computing_data_collection         'Bruker Duo'
_computing_cell_refinement         'Bruker Duo'
_computing_data_reduction          'Bruker Saint'
_computing_structure_solution      'SHELXS-97 (Sheldrick, 2008)'
_computing_structure_refinement    'SHELXL-97 (Sheldrick, 2008)'
_computing_molecular_graphics      'Bruker Shelxtl'
_computing_publication_material    'Bruker Shelxtl'

_refine_special_details
;
 Refinement of F^2^ against ALL reflections.  The weighted R-factor wR
and goodness of fit S are based on F^2^, conventional R-factors R are
based on F, with F set to zero for negative F^2^. The threshold
expression of F^2^ > 2sigma(F^2^) is used only for calculating R-
factors(gt) etc. and is not relevant to the choice of reflections for
refinement.  R-factors based on F^2^ are statistically about twice as
large as those based on F, and R- factors based on ALL data will be
even larger.

_refine_ls_structure_factor_coef  Fsqd
_refine_ls_matrix_type            full
_refine_ls_weighting_scheme       calc
_refine_ls_weighting_details
 'calc w=1/[\s^2^(Fo^2^)+(0.1224P)^2^+0.7618P] where
P=(Fo^2^+2Fc^2^)/3'
_atom_sites_solution_primary      direct
_atom_sites_solution_secondary    difmap
_atom_sites_solution_hydrogens    geom
_refine_ls_hydrogen_treatment     constr
_refine_ls_extinction_method      none
_refine_ls_extinction_coef        ?
_refine_ls_abs_structure_details
 'Flack H D (1983), Acta Cryst. A39, 876-881'
_refine_ls_abs_structure_Flack    0.15(3)
_refine_ls_number_reflns          8281
_refine_ls_number_parameters      443
_refine_ls_number_restraints      1
_refine_ls_R_factor_all           0.0720
_refine_ls_R_factor_gt            0.0706
_refine_ls_wR_factor_ref          0.1922
_refine_ls_wR_factor_gt           0.1907
_refine_ls_goodness_of_fit_ref    1.050
_refine_ls_restrained_S_all       1.050
_refine_ls_shift/su_max           0.000
_refine_ls_shift/su_mean          0.000

loop_
 _atom_site_label
 _atom_site_type_symbol
 _atom_site_fract_x
 _atom_site_fract_y
 _atom_site_fract_z
```

```
 _atom_site_U_iso_or_equiv
 _atom_site_adp_type
 _atom_site_occupancy
 _atom_site_symmetry_multiplicity
 _atom_site_calc_flag
 _atom_site_refinement_flags
 _atom_site_disorder_assembly
 _atom_site_disorder_group
Si1 Si 0.83466(8) 0.26003(3) 0.71798(6) 0.03155(18) Uani 1 1 d . . .
O5 O 0.8950(2) 0.25782(8) 0.58651(17) 0.0366(4) Uani 1 1 d . . .
O1 O 0.6806(2) 0.30151(7) 0.67662(18) 0.0352(4) Uani 1 1 d . . .
O2 O 0.6776(3) 0.22159(8) 0.6910(2) 0.0401(5) Uani 1 1 d . . .
O3 O 0.9516(3) 0.29991(8) 0.8166(2) 0.0405(5) Uani 1 1 d . . .
O4 O 0.9615(3) 0.21825(7) 0.80332(19) 0.0366(5) Uani 1 1 d . . .
C6 C 0.7264(4) 0.34282(11) 0.7341(2) 0.0342(6) Uani 1 1 d . . .
C7 C 0.8922(4) 0.17562(11) 0.7887(2) 0.0334(6) Uani 1 1 d . . .
C8 C 0.8064(3) 0.26247(13) 0.3676(3) 0.0398(6) Uani 1 1 d . . .
C9 C 0.6356(4) 0.13862(11) 0.6996(3) 0.0405(7) Uani 1 1 d . . .
H9A H 0.5247 0.1407 0.6545 0.049 Uiso 1 1 calc R . .
C10 C 0.7292(4) 0.17759(11) 0.7236(3) 0.0385(7) Uani 1 1 d . . .
C11 C 0.6290(4) 0.38119(11) 0.7208(3) 0.0403(7) Uani 1 1 d . . .
H11A H 0.5213 0.3807 0.6677 0.048 Uiso 1 1 calc R . .
O6 O 0.7886(3) 0.21652(9) 0.3680(2) 0.0532(6) Uani 1 1 d . . .
C13 C 0.8823(4) 0.34173(11) 0.8147(3) 0.0370(6) Uani 1 1 d . . .
C14 C 0.9646(4) 0.13436(12) 0.8348(3) 0.0425(7) Uani 1 1 d . . .
C15 C 0.7040(4) 0.09608(11) 0.7417(3) 0.0423(7) Uani 1 1 d . . .
C16 C 0.9494(4) 0.38094(12) 0.8827(3) 0.0462(7) Uani 1 1 d . . .
C18 C 0.8622(4) 0.28633(11) 0.4830(3) 0.0389(6) Uani 1 1 d . . .
C19 C 0.8691(5) 0.09575(12) 0.8092(3) 0.0492(8) Uani 1 1 d . . .
H19A H 0.9172 0.0669 0.8390 0.059 Uiso 1 1 calc R . .
C20 C 0.6946(4) 0.42106(11) 0.7885(3) 0.0438(7) Uani 1 1 d . . .
C21 C 0.8495(5) 0.41997(12) 0.8663(4) 0.0508(8) Uani 1 1 d . . .
H21A H 0.8917 0.4472 0.9117 0.061 Uiso 1 1 calc R . .
C22 C 1.2469(5) 0.15054(16) 0.8262(4) 0.0627(10) Uani 1 1 d . . .
H22A H 1.3613 0.1492 0.8731 0.094 Uiso 1 1 calc R . .
H22B H 1.2166 0.1825 0.8022 0.094 Uiso 1 1 calc R . .
H22C H 1.2270 0.1315 0.7500 0.094 Uiso 1 1 calc R . .
C23 C 0.8877(4) 0.33279(11) 0.4924(3) 0.0413(7) Uani 1 1 d . . .
H23A H 0.9283 0.3471 0.5726 0.050 Uiso 1 1 calc R . .
C24 C 0.7095(4) 0.26388(17) 0.1253(3) 0.0540(8) Uani 1 1 d . . .
C25 C 0.5959(5) 0.46614(12) 0.7793(4) 0.0540(9) Uani 1 1 d . . .
C26 C 1.1747(5) 0.16280(19) 1.0259(4) 0.0660(11) Uani 1 1 d . . .
H26A H 1.1114 0.1513 1.0798 0.099 Uiso 1 1 calc R . .
H26B H 1.1421 0.1945 0.9997 0.099 Uiso 1 1 calc R . .
H26C H 1.2892 0.1623 1.0729 0.099 Uiso 1 1 calc R . .
C27 C 1.1461(4) 0.13227(12) 0.9098(3) 0.0492(8) Uani 1 1 d . . .
C28 C 0.5527(5) 0.23897(19) 0.1181(4) 0.0678(12) Uani 1 1 d . . .
H28A H 0.5131 0.2236 0.0361 0.102 Uiso 1 1 calc R . .
H28B H 0.4726 0.2613 0.1280 0.102 Uiso 1 1 calc R . .
H28C H 0.5716 0.2160 0.1856 0.102 Uiso 1 1 calc R . .
C30 C 0.8377(6) 0.23158(18) 0.1083(4) 0.0683(11) Uani 1 1 d . . .
H30A H 0.7992 0.2161 0.0264 0.102 Uiso 1 1 calc R . .
```

```
H30B H 0.8621 0.2085 0.1758 0.102 Uiso 1 1 calc R . .
H30C H 0.9352 0.2492 0.1115 0.102 Uiso 1 1 calc R . .
C31 C 1.1705(7) 0.4271(2) 1.0374(7) 0.097(2) Uani 1 1 d . . .
H31A H 1.1606 0.4515 0.9745 0.145 Uiso 1 1 calc R . .
H31B H 1.2823 0.4253 1.0905 0.145 Uiso 1 1 calc R . .
H31C H 1.1003 0.4340 1.0902 0.145 Uiso 1 1 calc R . .
C33 C 0.8839(5) 0.41151(13) 0.3913(4) 0.0560(9) Uani 1 1 d . . .
C34 C 1.1987(6) 0.08290(17) 0.9510(5) 0.0779(14) Uani 1 1 d . . .
H34A H 1.1355 0.0712 1.0049 0.117 Uiso 1 1 calc R . .
H34B H 1.3131 0.0827 0.9982 0.117 Uiso 1 1 calc R . .
H34C H 1.1810 0.0632 0.8763 0.117 Uiso 1 1 calc R . .
C35 C 0.5701(6) 0.47647(15) 0.9074(4) 0.0653(11) Uani 1 1 d . . .
H35A H 0.6746 0.4791 0.9715 0.098 Uiso 1 1 calc R . .
H35B H 0.5083 0.4514 0.9304 0.098 Uiso 1 1 calc R . .
H35C H 0.5109 0.5055 0.9026 0.098 Uiso 1 1 calc R . .
C36 C 0.6881(7) 0.50573(14) 0.7397(5) 0.0730(13) Uani 1 1 d . . .
H36A H 0.7942 0.5088 0.8014 0.110 Uiso 1 1 calc R . .
H36B H 0.6279 0.5345 0.7361 0.110 Uiso 1 1 calc R . .
H36C H 0.7010 0.4991 0.6564 0.110 Uiso 1 1 calc R . .
C38 C 1.1397(7) 0.3435(2) 1.0705(5) 0.0866(17) Uani 1 1 d . . .
H38A H 1.1122 0.3135 1.0290 0.130 Uiso 1 1 calc R . .
H38B H 1.0676 0.3500 1.1221 0.130 Uiso 1 1 calc R . .
H38C H 1.2512 0.3428 1.1245 0.130 Uiso 1 1 calc R . .
C39 C 0.4297(6) 0.46213(14) 0.6812(5) 0.0688(12) Uani 1 1 d . . .
H39A H 0.3690 0.4370 0.7052 0.103 Uiso 1 1 calc R . .
H39B H 0.4434 0.4557 0.5980 0.103 Uiso 1 1 calc R . .
H39C H 0.3708 0.4911 0.6781 0.103 Uiso 1 1 calc R . .
C41 C 0.6770(6) 0.2986(2) 0.0176(3) 0.0727(13) Uani 1 1 d . . .
H41A H 0.6377 0.2824 -0.0632 0.109 Uiso 1 1 calc R . .
H41B H 0.7766 0.3150 0.0204 0.109 Uiso 1 1 calc R . .
H41C H 0.5957 0.3208 0.0262 0.109 Uiso 1 1 calc R . .
C42 C 0.6056(6) 0.05127(13) 0.7173(5) 0.0632(11) Uani 1 1 d . . .
C44 C 0.4426(7) 0.05715(15) 0.6239(7) 0.093(2) Uani 1 1 d . . .
H44A H 0.4550 0.0666 0.5422 0.139 Uiso 1 1 calc R . .
H44B H 0.3823 0.0808 0.6544 0.139 Uiso 1 1 calc R . .
H44C H 0.3840 0.0279 0.6141 0.139 Uiso 1 1 calc R . .
C45 C 0.7738(4) 0.28891(13) 0.2567(3) 0.0443(7) Uani 1 1 d . . .
C49 C 1.1213(5) 0.38109(16) 0.9705(4) 0.0631(11) Uani 1 1 d . . .
C50 C 0.8525(4) 0.35901(12) 0.3810(3) 0.0454(7) Uani 1 1 d . . .
C51 C 0.7967(4) 0.33592(13) 0.2659(3) 0.0479(8) Uani 1 1 d . . .
H51A H 0.7735 0.3535 0.1903 0.058 Uiso 1 1 calc R . .
C52 C 0.8202(10) 0.4359(2) 0.2646(6) 0.099(2) Uani 1 1 d . . .
H52A H 0.8427 0.4690 0.2758 0.149 Uiso 1 1 calc R . .
H52B H 0.7039 0.4311 0.2321 0.149 Uiso 1 1 calc R . .
H52C H 0.8732 0.4234 0.2047 0.149 Uiso 1 1 calc R . .
C58 C 0.6975(7) 0.01311(15) 0.6732(6) 0.0791(14) Uani 1 1 d . . .
H58A H 0.7143 0.0218 0.5924 0.119 Uiso 1 1 calc R . .
H58B H 0.6355 -0.0156 0.6628 0.119 Uiso 1 1 calc R . .
H58C H 0.8019 0.0085 0.7362 0.119 Uiso 1 1 calc R . .
C60 C 1.2352(6) 0.3710(2) 0.8879(6) 0.0857(16) Uani 1 1 d . . .
H60A H 1.2232 0.3953 0.8242 0.129 Uiso 1 1 calc R . .
H60B H 1.2074 0.3412 0.8458 0.129 Uiso 1 1 calc R . .
```

```
H60C H 1.3469 0.3703 0.9416 0.129 Uiso 1 1 calc R . .
C53 C 0.8044(11) 0.43254(19) 0.4803(8) 0.112(3) Uani 1 1 d . . .
H53A H 0.8427 0.4173 0.5626 0.168 Uiso 1 1 calc R . .
H53B H 0.6877 0.4287 0.4471 0.168 Uiso 1 1 calc R . .
H53C H 0.8305 0.4654 0.4898 0.168 Uiso 1 1 calc R . .
C54 C 1.0616(8) 0.4199(2) 0.4355(9) 0.117(3) Uani 1 1 d . . .
H54A H 1.1075 0.4045 0.5168 0.176 Uiso 1 1 calc R . .
H54B H 1.0821 0.4531 0.4453 0.176 Uiso 1 1 calc R . .
H54C H 1.1114 0.4076 0.3733 0.176 Uiso 1 1 calc R . .
C59 C 0.5758(8) 0.03591(17) 0.8432(6) 0.0851(16) Uani 1 1 d . . .
H59A H 0.5124 0.0074 0.8294 0.128 Uiso 1 1 calc R . .
H59B H 0.5171 0.0601 0.8730 0.128 Uiso 1 1 calc R . .
H59C H 0.6793 0.0305 0.9067 0.128 Uiso 1 1 calc R . .

loop_
 _atom_site_aniso_label
 _atom_site_aniso_U_11
 _atom_site_aniso_U_22
 _atom_site_aniso_U_33
 _atom_site_aniso_U_23
 _atom_site_aniso_U_13
 _atom_site_aniso_U_12
Si1 0.0267(3) 0.0375(3) 0.0269(3) 0.0033(3) 0.0021(2) 0.0009(3)
O5 0.0366(10) 0.0400(9) 0.0326(9) 0.0025(9) 0.0092(7) 0.0040(9)
O1 0.0286(11) 0.0401(11) 0.0324(9) -0.0039(9) 0.0017(8) 0.0009(8)
O2 0.0264(11) 0.0410(11) 0.0469(12) 0.0104(9) 0.0011(8) 0.0046(8)
O3 0.0286(12) 0.0486(12) 0.0379(10) 0.0019(9) -0.0005(8) -0.0012(8)
O4 0.0291(12) 0.0445(11) 0.0318(10) 0.0078(8) 0.0016(8) 0.0056(8)
C6 0.0401(17) 0.0418(14) 0.0213(12) -0.0045(11) 0.0100(10) -0.0056(12)
C7 0.0339(16) 0.0449(15) 0.0203(12) -0.0021(10) 0.0063(10) 0.0025(11)
C8 0.0318(14) 0.0503(16) 0.0382(14) 0.0044(14) 0.0115(10) 0.0082(14)
C9 0.0323(17) 0.0448(17) 0.0442(16) 0.0000(13) 0.0107(12) 0.0023(12)
C10 0.0380(18) 0.0379(15) 0.0388(15) 0.0051(12) 0.0097(12) 0.0060(12)
C11 0.0416(18) 0.0409(15) 0.0379(15) -0.0028(12) 0.0103(12) -
0.0026(12)
O6 0.0620(17) 0.0538(14) 0.0425(12) -0.0055(10) 0.0130(11) -0.0063(11)
C13 0.0391(18) 0.0443(15) 0.0273(13) 0.0034(12) 0.0092(11) -0.0072(12)
C14 0.0410(18) 0.0523(17) 0.0333(15) 0.0055(13) 0.0095(12) 0.0124(13)
C15 0.052(2) 0.0380(15) 0.0358(15) -0.0034(12) 0.0116(13) 0.0055(13)
C16 0.0413(19) 0.0494(17) 0.0442(17) -0.0054(14) 0.0065(13) -
0.0147(13)
C18 0.0266(15) 0.0525(17) 0.0368(15) 0.0031(12) 0.0077(11) 0.0041(11)
C19 0.057(2) 0.0427(16) 0.0460(18) 0.0113(14) 0.0114(15) 0.0170(14)
C20 0.050(2) 0.0411(16) 0.0428(17) -0.0017(13) 0.0169(13) -0.0074(13)
C21 0.057(2) 0.0415(16) 0.0497(19) -0.0126(14) 0.0092(15) -0.0124(14)
C22 0.041(2) 0.071(2) 0.074(3) 0.015(2) 0.0141(17) 0.0210(17)
C23 0.0364(17) 0.0502(17) 0.0378(15) 0.0002(13) 0.0117(12) 0.0027(12)
C24 0.0400(17) 0.085(2) 0.0348(15) 0.0010(18) 0.0070(11) -0.0044(18)
C25 0.065(3) 0.0401(17) 0.055(2) -0.0068(15) 0.0131(17) 0.0010(15)
C26 0.049(2) 0.100(3) 0.0380(18) 0.0050(19) -0.0043(15) 0.014(2)
C27 0.041(2) 0.0533(19) 0.0440(18) 0.0081(15) -0.0030(13) 0.0156(14)
C28 0.047(2) 0.109(3) 0.0431(19) -0.014(2) 0.0076(15) -0.015(2)
```

```
C30 0.071(3) 0.086(3) 0.051(2) -0.012(2) 0.0227(19) 0.001(2)
C31 0.061(3) 0.081(3) 0.119(5) -0.043(3) -0.020(3) -0.019(2)
C33 0.066(3) 0.0507(19) 0.054(2) 0.0119(16) 0.0231(17) 0.0062(16)
C34 0.057(3) 0.069(3) 0.094(3) 0.034(3) 0.000(2) 0.024(2)
C35 0.076(3) 0.054(2) 0.068(3) -0.0112(19) 0.024(2) 0.0028(18)
C36 0.099(4) 0.0394(19) 0.083(3) -0.0021(19) 0.031(3) -0.002(2)
C38 0.074(3) 0.089(3) 0.065(3) -0.006(2) -0.032(2) -0.014(2)
C39 0.075(3) 0.047(2) 0.077(3) -0.006(2) 0.011(2) 0.0146(19)
C41 0.065(3) 0.118(4) 0.0307(16) -0.002(2) 0.0065(15) 0.004(2)
C42 0.066(3) 0.0362(17) 0.084(3) -0.0018(18) 0.017(2) 0.0031(16)
C44 0.070(3) 0.042(2) 0.146(6) -0.009(3) 0.000(3) -0.0115(19)
C45 0.0379(17) 0.067(2) 0.0295(14) 0.0046(13) 0.0120(11) 0.0082(14)
C49 0.049(2) 0.066(2) 0.064(2) -0.015(2) -0.0009(18) -0.0166(17)
C50 0.0425(18) 0.0539(18) 0.0425(16) 0.0010(14) 0.0164(13) 0.0064(13)
C51 0.0397(18) 0.059(2) 0.0464(18) 0.0080(15) 0.0143(13) 0.0059(14)
C52 0.157(7) 0.065(3) 0.086(4) 0.019(3) 0.052(4) 0.014(3)
C58 0.084(4) 0.045(2) 0.109(4) -0.019(2) 0.030(3) 0.000(2)
C60 0.050(3) 0.087(4) 0.110(4) -0.025(3) 0.007(3) -0.015(2)
C53 0.169(7) 0.052(3) 0.145(6) 0.018(3) 0.094(6) 0.017(3)
C54 0.086(5) 0.065(3) 0.193(8) 0.019(4) 0.027(5) -0.018(3)
C59 0.100(4) 0.052(2) 0.115(4) 0.011(3) 0.049(3) -0.007(2)

_geom_special_details
;
 All esds (except the esd in the dihedral angle between two l.s.
planes) are estimated using the full covariance matrix.  The cell esds
are taken into account individually in the estimation of esds in
distances, angles and torsion angles; correlations between esds in
cell parameters are only used when they are defined by crystal
symmetry.  An approximate (isotropic) treatment of cell esds is used
for estimating esds involving l.s. planes.

loop_
 _geom_bond_atom_site_label_1
 _geom_bond_atom_site_label_2
 _geom_bond_distance
 _geom_bond_site_symmetry_2
 _geom_bond_publ_flag
Si1 O5 1.684(2) . ?
Si1 O3 1.709(2) . ?
Si1 O2 1.720(2) . ?
Si1 O4 1.725(2) . ?
Si1 O1 1.759(2) . ?
O5 C18 1.375(4) . ?
O1 C6 1.361(4) . ?
O2 C10 1.367(4) . ?
O3 C13 1.352(4) . ?
O4 C7 1.365(4) . ?
C6 C11 1.380(5) . ?
C6 C13 1.390(4) . ?
C7 C14 1.380(4) . ?
C7 C10 1.392(4) . ?
```

```
C8 O6 1.342(5) . ?
C8 C45 1.405(4) . ?
C8 C18 1.410(4) . ?
C9 C10 1.373(5) . ?
C9 C15 1.391(5) . ?
C11 C20 1.406(5) . ?
C13 C16 1.395(4) . ?
C14 C19 1.374(5) . ?
C14 C27 1.556(5) . ?
C15 C19 1.412(5) . ?
C15 C42 1.537(5) . ?
C16 C21 1.406(6) . ?
C16 C49 1.528(5) . ?
C18 C23 1.365(5) . ?
C20 C21 1.372(5) . ?
C20 C25 1.551(5) . ?
C22 C27 1.540(6) . ?
C23 C50 1.405(5) . ?
C24 C30 1.509(6) . ?
C24 C41 1.524(6) . ?
C24 C28 1.523(6) . ?
C24 C45 1.577(5) . ?
C25 C35 1.528(6) . ?
C25 C36 1.534(6) . ?
C25 C39 1.540(6) . ?
C26 C27 1.521(6) . ?
C27 C34 1.533(5) . ?
C31 C49 1.527(6) . ?
C33 C53 1.487(8) . ?
C33 C54 1.498(8) . ?
C33 C52 1.525(7) . ?
C33 C50 1.546(5) . ?
C38 C49 1.529(7) . ?
C42 C44 1.502(7) . ?
C42 C58 1.526(6) . ?
C42 C59 1.555(8) . ?
C45 C51 1.378(5) . ?
C49 C60 1.558(8) . ?
C50 C51 1.397(5) . ?

loop_
 _geom_angle_atom_site_label_1
 _geom_angle_atom_site_label_2
 _geom_angle_atom_site_label_3
 _geom_angle
 _geom_angle_site_symmetry_1
 _geom_angle_site_symmetry_3
 _geom_angle_publ_flag
O5 Si1 O3 107.57(12) . . ?
O5 Si1 O2 104.72(12) . . ?
O3 Si1 O2 147.69(12) . . ?
O5 Si1 O4 97.89(11) . . ?
```

```
O3 Si1 O4 87.61(9) . . ?
O2 Si1 O4 89.32(11) . . ?
O5 Si1 O1 101.79(10) . . ?
O3 Si1 O1 88.29(10) . . ?
O2 Si1 O1 83.88(9) . . ?
O4 Si1 O1 160.22(11) . . ?
C18 O5 Si1 130.98(19) . . ?
C6 O1 Si1 112.55(19) . . ?
C10 O2 Si1 112.2(2) . . ?
C13 O3 Si1 114.68(19) . . ?
C7 O4 Si1 112.46(19) . . ?
O1 C6 C11 125.0(3) . . ?
O1 C6 C13 112.3(3) . . ?
C11 C6 C13 122.7(3) . . ?
O4 C7 C14 127.2(3) . . ?
O4 C7 C10 111.9(3) . . ?
C14 C7 C10 120.9(3) . . ?
O6 C8 C45 123.5(3) . . ?
O6 C8 C18 119.6(3) . . ?
C45 C8 C18 116.9(3) . . ?
C10 C9 C15 119.6(3) . . ?
O2 C10 C9 126.0(3) . . ?
O2 C10 C7 112.4(3) . . ?
C9 C10 C7 121.6(3) . . ?
C6 C11 C20 117.7(3) . . ?
O3 C13 C6 112.2(3) . . ?
O3 C13 C16 127.5(3) . . ?
C6 C13 C16 120.4(3) . . ?
C19 C14 C7 116.6(3) . . ?
C19 C14 C27 122.4(3) . . ?
C7 C14 C27 120.9(3) . . ?
C9 C15 C19 117.0(3) . . ?
C9 C15 C42 122.0(3) . . ?
C19 C15 C42 121.0(3) . . ?
C13 C16 C21 116.2(3) . . ?
C13 C16 C49 121.7(3) . . ?
C21 C16 C49 122.2(3) . . ?
C23 C18 O5 122.7(3) . . ?
C23 C18 C8 124.0(3) . . ?
O5 C18 C8 113.2(3) . . ?
C14 C19 C15 124.3(3) . . ?
C21 C20 C11 119.2(3) . . ?
C21 C20 C25 118.9(3) . . ?
C11 C20 C25 121.8(3) . . ?
C20 C21 C16 123.8(3) . . ?
C18 C23 C50 118.6(3) . . ?
C30 C24 C41 106.8(3) . . ?
C30 C24 C28 112.3(4) . . ?
C41 C24 C28 108.2(3) . . ?
C30 C24 C45 108.9(3) . . ?
C41 C24 C45 110.7(4) . . ?
C28 C24 C45 109.9(3) . . ?
```

```
C35 C25 C36 110.3(4) . . ?
C35 C25 C39 108.1(4) . . ?
C36 C25 C39 108.4(4) . . ?
C35 C25 C20 109.3(3) . . ?
C36 C25 C20 109.0(4) . . ?
C39 C25 C20 111.7(3) . . ?
C26 C27 C34 109.3(4) . . ?
C26 C27 C22 108.9(4) . . ?
C34 C27 C22 109.2(4) . . ?
C26 C27 C14 108.7(3) . . ?
C34 C27 C14 111.4(3) . . ?
C22 C27 C14 109.3(3) . . ?
C53 C33 C54 110.4(6) . . ?
C53 C33 C52 107.7(5) . . ?
C54 C33 C52 106.9(5) . . ?
C53 C33 C50 110.3(4) . . ?
C54 C33 C50 109.1(4) . . ?
C52 C33 C50 112.4(4) . . ?
C44 C42 C58 109.8(5) . . ?
C44 C42 C15 113.0(3) . . ?
C58 C42 C15 110.7(4) . . ?
C44 C42 C59 106.4(5) . . ?
C58 C42 C59 108.4(4) . . ?
C15 C42 C59 108.2(4) . . ?
C51 C45 C8 119.2(3) . . ?
C51 C45 C24 121.9(3) . . ?
C8 C45 C24 118.8(3) . . ?
C16 C49 C38 109.7(3) . . ?
C16 C49 C31 113.4(4) . . ?
C38 C49 C31 108.5(4) . . ?
C16 C49 C60 107.2(4) . . ?
C38 C49 C60 109.8(5) . . ?
C31 C49 C60 108.2(4) . . ?
C51 C50 C23 118.1(3) . . ?
C51 C50 C33 123.2(3) . . ?
C23 C50 C33 118.7(3) . . ?
C45 C51 C50 123.1(3) . . ?

_diffrn_measured_fraction_theta_max    0.960
_diffrn_reflns_theta_full              70.08
_diffrn_measured_fraction_theta_full   0.960
_refine_diff_density_max    0.531
_refine_diff_density_min   -0.292
_refine_diff_density_rms    0.068
```

Appendix C

The full SUP file for the crystallographic structure of $[(cat)_2Si(catH)][Et_3N]$ contains extensive detail of the x,y, and z coordinates for the location of each atom. This extended file has been appropriately stored in the Berben Group Lab Computer within the master 'Filed Theses' section of the group's filing system and can be found accordingly for further use or compound reproduction.